UNITED STATES DEPARTMENT OF THE INTERIOR
GEOLOGICAL SURVEY

Earthquake Hazards in the Pacific Northwest of the United States

Compiled by
A. M. Rogers
T. J. Walsh
W. J. Kockelman
G. R. Priest

GIS Applications in Seismic Loss Estimation Model For Portland, Oregon Water and Sewer Systems

By Leon R.L. Wang[1], Joyce C.C. Wang[2], and Isao Ishibashi[1]

Open-File Report 91-441-F

[1]Professor of Civil Engineering, Old Dominion University, Norfolk, VA 23529
[2]Adjunct Faculty, Old Dominion University

1991

Foreword

This paper is one of a series dealing with earthquake hazards of the Pacific Northwest, primarily in western Oregon and western Washington. This research represents the efforts of U.S. Geological Survey, university, and industry scientists in response to the Survey initiatives under the National Earthquake Hazards Reduction Program. Subject to Director's approval, these papers will appear collectively as U.S. Geological Survey Professional Paper 1560, tentatively titled "Assessing and Reducing Earthquake Hazards in the Pacific Northwest." The U.S. Geological Survey Open-File series will serve as a preprint for the Professional Paper chapters that the editors and authors believe require early release. A single Open-File will also be published that includes only the abstracts of those papers not included in the pre-release. The papers to be included in the Professional Paper are:

Introduction

Rogers, A.M., Walsh, T.J., Kockelman, W.J., and Priest, G.R., "Assessing and reducing earthquake hazards in the Pacific Northwest: An overview

Tectonic Setting

Paleoseismicity

Adams, John, "Great earthquakes recorded by turbidites off the Oregon-Washington margin"

Atwater, Brian, "Coastal evidence for great earthquakes in western Washington"

Nelson, Alan R. and Personius, Stephen F., "The potential for great earthquakes in Oregon and Washington: An overview of recent coastal geologic studies and their bearing on segmentation of Holocene ruptures, central Cascadia subduction zone"

Peterson, C. D. and Darienzo, M. E., "Discrimination of climatic, oceanic, and tectonic forcing of marsh burial events from Alsea Bay, Oregon, U.S.A."

Tectonics/Geophysics

Goldfinger, C. Kulm, V., Yeats, R., Appelgate, B., MacKay, M., and Cochrane, G., "Active strike slip faulting and folding in the Cascadia plate boundary and forearc, in central and northern Oregon"

Ma, Li, Crosson, Robert, and Ludwin, Ruth, "Focal mechanisms of western Washington earthquakes and their relationship to regional tectonic stress"

Snavely, P. D., Jr., "Cenozoic evolution of the continental margin of Oregon and Washington"

Weaver, C. S. and Shedlock, K. M., "Estimates of seismic source regions from considerations of the earthquake distribution and regional tectonics"

Yeats, Robert, Graven, E.P., Werner, K.S., Goldfinger, C., and Popowski, T, "Tectonic setting of the Willamette Valley, Oregon"

Earthquake Hazards

Ground Motion Prediction

Cohee, B.P., Sommerville, P.G., Abrahamson, N.A., "Ground motions from simulated Mw=8 Cascadia earthquakes"

King, Kenneth, Carver, D., Williams, R., Worley, D., "Site response studies in west and south Seattle, Washington"

Madin, Ian P., "Earthquake-hazard geology maps of the Portland metropolitan area, Oregon"

Silva, Walter, Wong, Ivan, and Darragh, Robert, "Engineering characterization of strong ground motions with applications to the Pacific Northwest"

Ground Failure

Chleborad, A. F. and Schuster, R. L., "Earthquake-induced ground failure associated with the April 13, 1949, and April 29, 1963, Puget Sound area, Washington, earthquakes"

Grant, W. P., Perkins, W. J., and Youd, L., "Liquefaction susceptibility maps for Seattle, Washington North and South Quadrangles

Earthquake Risk Assessment

Wang, Leon R.L., Wang, Joyce C.C., and Ishibashi, Isao, "GIS applications in seismic loss estimation model for Portland, Oregon water and sewer systems"

Implementation

Kockelman, William J., "Techniques for reducing earthquake hazards--An introduction"

Booth, Derek and Bethel, John, "Approaches for seismic hazard mitigation by local governments--An example from King County, Washington"

May, P.J., "Earthquake risk reduction prospects for the Puget Sound and Portland Areas"

Perkins, J.B. and Moy, K.K., "Liability for earthquake hazards or losses and its impacts on Washington's cities and counties"

Preuss, Jane and Hebenstreit, G. T., "Integrated hazard assessment for a coastal community: Grays Harbor"

Contents

List of Tables

ILLUSTRATIONS

ABSTRACT

Water and sanitary sewer systems are vital lifelines for cities and towns. These systems have been damaged by recent earthquakes including the recent Loma Prieta, California earthquake of October 17, 1989. The damage of a water system would hamper the fire-fighting capability and the damage of a sanitary sewer system could cause health problems. Both systems need protection against a major earthquake, and the mitigation of earthquake damage to water and sewer systems becomes local and regional concerns.

Portland, Oregon has been identified by USGS as one of the earthquake-prone areas that needs an earthquake hazard mitigation. This project develops an efficient and realistic seismic loss-estimation model for the water and sanitary sewer systems using Portland, Oregon as an example. The model can also be applied to other communities within earthquake-prone regions of the country to assist in the earthquake hazard mitigation of water/sewer lifelines.

The scope of the project consists of (1) the development of a methodology for the inventory of water and sewer systems using GIS (Geographic Information System) technology for a timely retrieval of statistical reports and spatial depiction of affected network and areas, (2) the formulation of a simple semi-empirical loss-estimation algorithm for the damage to such lifeline systems under different levels of earthquake ground shaking, and (3) the demonstration of the efficient display of loss-estimation algorithm by using two specific sewage drainage basins in Portland which contain important water and sewerage facilities.

For seismic applications, two earthquake scenarios, one local and one subduction, have been applied to the loss-estimation algorithm to estimate the pipeline damage in the two demonstrated drainage basins. Both earthquake shaking and soil liquefaction effects have been considered in the analysis.

A semi-empirical seismic loss algorithm for buried pipelines (both water and sewer) has been developed for various earthquake intensities. The model includes such parameters as soil conditions, pipe materials, and joint properties. Using this model, the loss and replacement costs under an earthquake scenario can be estimated and displayed by the GIS systems. The affected areas can also be displayed.

PC- and workstation-based hardwares have been used to demonstrate the feasibility and applicability of the project to a small or moderate-sized city. Two relatively easy operational GIS software packages are used for the availability and affordability reasons.

The GIS model developed using a PC or a workstation can help the small to moderate-sized city to conduct pre-earthquake planning, to identify the affected areas from breakage(s) reported in the network systems during the earthquake, and to set a priority for a post-earthquake damage survey, repair, or restoration under the emergency situation.

INTRODUCTION

Water and Sanitary sewer systems are vital lifelines for cities and towns. Recent Studies (Kubo and Isoyama, 1980; Wang, Sun, and Shen, 1985) have shown that water and sewer systems have been damaged by earthquakes including the recent Loma Prieta, California earthquake of October 17, 1989 (EERI, 1989). Because of the breakage of water mains, fires burned extensive portions of the cities of San Francisco in 1906 and Tokyo in 1923. The spread of disease could become epidemic due to the breakage of sanitary sewer lines during earthquakes. Thus, the protection of water and sewer systems becomes local and regional concerns and is urgently needed.

While a seismic code for water or sewer systems is not available in the United States at the present time, some counter-measures have been suggested (Wang, 1988; Ballantyne et al., 1980). An ASCE Advisory Note on Lifeline Earthquake Engineering has been published (ASCE/TCLEE, 1983). However, very little practical work has been done for specific sites.

Some urbanized earthquake-prone areas in the country have initiated rigorous earthquake damage mitigation planning. The East Bay Municipal Utility District (EBMUD) in Oakland, California has a strong on-going earthquake hazards mitigation program. The State of California has outstanding earthquake preparedness projects such as SCEPP (Southern California Earthquake Preparedness Project) and BAREPP (Bay Area Regional Earthquake Preparedness Project).

Recently under the USGS National Earthquake Hazards Reduction Program (NEHRP), a project to study an earthquake risk to Utah water and gas systems by Taylor et al. (1988) and a project to study earthquake loss estimation modeling of the Seattle water system by Ballantyne (1989) have been initiated. In addition to California and Utah, Seattle, Washington and Portland, Oregon have been identified by USGS as earthquake-prone areas that also need the attention for earthquake hazard mitigation planning.

The Portland Bureau of Water Works (figure 1) is the largest supplier of potable water in the State of Oregon and provides domestic water to about 25% of the population in the state. Providing an earthquake loss estimation modeling of Portland water and sewer systems will assist the City to effectively conduct pre-earthquake planning and to demonstrate its techniques and usefulness to lifeline communities in the nation.

The goal of this project is to develop a realistic loss estimation model coupled with efficient GIS functionalities using a personal computer (PC) or a workstation for the Portland, Oregon water and sewer systems.

The objectives of the project are: (1) to assist the City of Portland and its surrounding areas in pre-earthquake planning by showing the potential losses to the water and sewer systems, (2) to help post-earthquake emergency repair and/or restoration of the damaged system(s) by showing the disaster-affected areas, and (3) to provide a workable model for other cities and towns in earthquake-prone areas to adopt this relatively easy operational model for earthquake hazard mitigation planning/action.

The methodology for inventory with the display of water and sewer systems is to use the tool of GIS (Geographic Information System) for timely retrieval of data and spatial identification of affected network. Two applicable GIS software packages have been chosen for this project because they are available and relatively inexpensive. One is called FMS/AC (Facility Mapping Systems, Inc., 1989) and the other is Geo/SQL (Generation 5 Technology, Inc., 1989). The GIS-based model would assist a community to evaluate effectively its current water and sewer network potential loss in a hazardous earthquake.

The reliable but simple loss-estimation algorithm for estimating the damage to buried lifeline systems under different levels of earthquake ground shaking is a semi-empirical approach. Specific applications have been demonstrated by investigating two typical sewage drainage basins (Tanner and Fiske) in Portland. Each of these basins contains important water and sewerage facilities.

The scope of the paper describes (1) the development of a methodology for inventory with the display of water and sewer systems using GIS technology, (2) the development of the semi-empirical loss algorithm for buried pipelines, (3) the evaluation of seismic and geotechnical conditions of the site, and (4) the application of them to Portland water and sewer systems.

Two GIS software packages, running on a PC and workstation, were used to demonstrate the feasibility, applicability and cost-effectiveness of the project to a small or moderate-sized city. For seismic applications, two earthquake scenarios; one local and one subduction, have been applied to the loss-estimation algorithm to estimate the pipeline damage in the two drainage basins. Both earthquake shaking and soil liquefaction effects have been considered in this analysis.

STUDY AREAS

Figure 1 shows the water source and delivery system for the City of Portland. A watershed of more than 100 square miles in size located 25-miles east of Portland is the primary water source. An emergency and back-up source has been developed using groundwaters of the Columbia River and several large capacity wells, and pumping facilities. Most of the Portland water system is supplied by gravity. Terminal reservoirs on the west side of the Willamette River represent the end of gravity supply. These terminal reservoirs serve the downtown central business district. Water for higher elevations is served through pump stations and storage tanks.

The Portland system of sanitary sewers consists of a wide range of sewer pipe sizes and types that collect sewage by gravity from homes and businesses and convey it to sewage lift stations that in turn convey the sewage to interceptors, larger pipelines and eventually to sewage treatment plants. The sewage systems include concrete, clay, brick and metallic pipes.

To demonstrate the approach for the inventory and analysis, the study focuses on two areas that include important water and sewage facilities and different characters of land use. These are also representative of different types of Portland geography.

TANNER DRAINAGE BASIN

The Tanner Drainage Basin is on the southwest side of the Willamette River. It includes a portion of the downtown area and follows westerly along Highway 26. The Tanner basin incorporates a large portion of Portland's central business district and residential areas. The Tanner Basin was selected for this study because of the variety of systems.

FISKE DRAINAGE BASIN

The Fiske Drainage Basin is bounded on the southwest by the Willamette River and, the northeast by the Columbia Slough. The Fiske Drainage Basin was selected because it includes the Columbia Boulevard Treatment Plant plus several storage tanks.

DEVELOPMENT OF A LOSS ALGORITHM FOR BURIED PIPELINES

BASIC DATA

This section develops a method for combining both analysis and data in order to derive illustrative and preliminary loss algorithms for damaged pipelines. Some of the problems in deriving these loss algorithms are indicated in this section. Note that alternative methods (Rojahn and Sharpe, 1985; Eguchi, et al., 1982) are available in the literature, which should be consulted in the development of loss algorithms to actual pipeline networks.

Seismic vulnerability and loss estimation models have been developed by several investigators including Eguchi (1983), Taylor, et al. (1986), and Wang (1979). The development of this preliminary loss algorithm (percentage loss or dollar loss versus Modified Mercalli Intensity, (MMI)) for application to seismic risk analysis is based on the statistics for buried pipelines compiled and interpreted by Katayama, et al. (1975) and others as indicated in figure 2. The data in the figure represent the repairs per kilometer of buried pipelines versus peak ground acceleration (PGA) from many earthquakes around the world. The damage has been classified for different soil conditions (poor, average and good) which are based on subjective judgment. However, no distinctions are made with reference to pipe materials, (e.g. cast iron, concrete, reinforced or prestressed concrete, steel, asbestos, plastics, etc.), pipe diameter, pipe type (segmented or continuous) or types of failure (axial, bending, shear, etc.). Readers should carefully scrutinize them before making any application, especially for earthquake scenarios with high peak ground accelerations affecting pipelines with poor soil conditions. A realistic upper bound on expected numbers of breaks per kilometer has been set at 15.0 in this project in order to avoid physically unreasonable extrapolations from the data.

Since the available data is not enough to perform various correlation analyses, the following assumptions for a referenced (average) condition are made in order to develop a robust loss algorithm for a wider range of applications.

1. Pipeline repair data are considered to be the same as pipeline damage data due to earthquakes.
2. Referenced (average) conditions;
   Material : Cast Iron
   Failure Strain : $\varepsilon_f = 0.003$
   Diameter : ϕ = 12 inches (30 cm)
   Length : L = 20 feet (6.5m)
   Type : Segmented
   Max. Joint Displ. : d_f = 1 inch (25 mm)
3. Soil conditions (in terms of typical shear wave propagation speed);
   Poor : 500 ft/sec (150 m/sec) or lower
   Average : 2000 ft/sec (600 m/sec) 500 ft/sec (150 m/sec)
   Good : 6000 ft/sec(1800 m/sec) or higher
4. Average year of construction - 1950.

Using data in figure 2, the equations for pipeline damage (breaks/km) versus peak ground acceleration (g) are as following:

For a poor soil condition
$\text{Log } Y = 6.4241 \text{ Log } A + 4.822;$ up to 15 breaks/km (1)

For an average soil condition
$\text{Log } Y = 6.0051 \text{ Log } A + 3.434;$ up to 15 breaks/km (2)

For a good soil condition
$\text{Log } Y = 5.3221 \text{ Log } A + 1.602;$ up to 15 breaks/km (3)

where Y is breaks/km, and A is peak ground acceleration in fraction of the gravitational acceleration.

PIPELINE DAMAGE (BREAKS/KM OR PERCENTAGE LOSS) VERSUS EARTHQUAKE INTENSITY (MMI)

Since damage relationships are typically described in terms of an intensity scale while attenuation relationships are defined in terms of strong motion data, it is frequently necessary to relate the two for seismic risk and other studies. As a result of these conversion needs, various investigators have developed alternative intensity conversion formulae.

Using the following conservative relationship between Modified Mercalli Intensity (MMI) scale and peak ground acceleration (g) proposed by Wiggins and Taylor (1986) for the demonstration purpose as:

$$\text{Log } A = -2.940 + 0.286 \, I \qquad (4)$$

Using above relationship, figure 2 can be reconstructed to show the pipeline damage (breaks/km) versus MMI relations as indicated in figure 3. The correlation equations are given below:

For a poor soil condition
$\text{Log } Y = 1.837 \, I - 14.065;$ $Y \leq 15$ (5)

For an average soil condition
$\text{Log } Y = 1.717 \, I - 14.221;$ $Y \leq 15$ (6)

For a good soil condition
$\text{Log } Y = 1.522 \, I - 14.005;$ $Y \leq 15$ (7)

where I is MMI intensity.

Please note that figure 3 shows straight lines plotted on a semi-log scale. The straight line equations (Eqns 5,6, and 7) may be used as a basis for modification of other parameters in terms of breaks/km.

If each pipe section is assumed to be approximately 20 ft (6.5 m), then there are approximately 150 pipe sections in a kilometer. It is likely that if breaks exceed a certain number within a specific kilometer then the entire pipe length will be replaced. On the other hand, costs for repairing some pipe breaks and leaks is far less than the cost for replacement of one section of pipe. A further complication is that several leaks may occur within the same section of a pipe. These and other complications would need to be considered in a more precise analysis of pipeline repair costs from earthquakes. As a result of the previous assumption that a maximum of 15 repairs are physically reasonable for a kilometer of pipe, a maximum of 10% replacement cost to pipelines has been assumed. These limits are illustrative of the decisions faced in applications to existing systems. Since only a very small percentage of pipelines are replaced in existing systems in the course of a normal maintenance in a year, the small percents referred to here may, in some cases, far exceed normal annual replacement rates. Therefore, figure 4 shows the percentage loss versus intensity as a measure for loss estimation of buried pipelines. The equations governing these percentage loss are shown below:

For a poor soil condition
$\text{Log } \bar{Y} = 1.837 \, I - 16.241;$ $\bar{Y} \leq 0.1$ (8)

For an average soil condition
$\text{Log } \bar{Y} = 1.717\, I - 16.397;$ $\bar{Y} \leq 0.1$ (9)

For a good soil condition
$\text{Log } \bar{Y} = 1.522\, I - 16.221;$ $\bar{Y} \leq 0.1$ (10)

where $\bar{Y}$ is a percentage loss, which will be used for this project study. These equations are considered as the referenced or basic loss algorithms for buried pipelines.

PARAMETRIC PIPELINE DAMAGE (PERCENT LOSS) VERSUS EARTHQUAKE INTENSITY (MMI)

To extend the basic empirical information to include such parameters as pipe material, year and type of construction and other soil conditions, we propose to modify the slopes and the constants of the above-mentioned basic loss algorithms (Eqns 8, 9, and 10) for various parameters by the following general equation:

$$\text{Log } \bar{Y} = \alpha_s a_o I - \beta_s b_o - \beta \tag{11}$$

where α_s is the modifier for the slope due to the change of soil condition, a_o is the slope and b_o is the constant of the loss algorithm for the average soil condition, β_s is the modifier for soil, and β, the modifier for the constant which is defined as:

$$\beta = \text{Log } (\beta_m \cdot \beta_j \cdot \beta_y) \tag{12}$$

in which β_m is the modifier for material ductility, β_j for type of construction and β_y for the year of construction.

For this study, only the soil condition, pipe material, type of construction and year of construction will be considered. However, for any other influential parameter, same procedure can be applied without difficulty.

Modifications for Soil Condition, α_s and β_s

From the damage statistics shown in figures 2 to 4, one notices that both the slopes and the constants are changed for different soil conditions. To include various soils (in terms of shear wave propagation speed) in the loss algorithm, both the slope and the constant will have to be modified. The modifications will be based on a linear interpolation from an average soil condition to a poor soil condition and from average to good condition for the referenced values assumed earlier.

Based on the damage statistics (fig. 3) and the assumed average conditions, the following constant variables are obtained.

C_s = 150 m/sec or less	$a_o^- = 1.837$	for poor soil condition
$C_s \simeq 600$ m/sec	$a_o = 1.717$	for average soil condition
C_s = 1800 m/sec or more	$a_o^+ = 1.522$	for good soil condition

where C_s is shear wave propagation speed.

By linear interpolation, the change of the slope from average to poor soil condition, $\alpha_s^- a_o$ is shown below, where α_s^- is the modifier and $a_o = 1.717$ is the slope of the loss algorithm for the average soil condition.

$$\frac{\alpha_s^- a_o - a_o}{600 - C_s} = \frac{a_o^- - a_o}{600 - 150} = \frac{1.837 - 1.717}{600 - 150} = 0.000267 \tag{13}$$

From Eqn (13) and $a_o = 1.717$, α_s^- can be determined as:

$$\alpha_s^- = 1.093 - 1.556 \times 10^{-4}\, C_s \tag{14}$$

Similarly, the modifier for the slope from average to good soil condition, α^+_s is determined as:

$$\alpha_s^{+} = 1.057 - 9.5 \times 10^{-5}\, C_s \qquad (15)$$

The linear interpolation is graphically shown in figure 5. Note that since the slopes of the algorithms based on the breaks/km or percentage loss are the same, no additional work is needed.

Using the same linear interpolation scheme, the modification equations of constant term in the algorithm for soil properties are given below without further explanation.

	Breaks/km Loss Algorithm;	Percentage Loss Algorithm	
From average to poor soil condition	$\beta_s^{-} = 0.985374 + 24.4 \times 10^{-6} C_s$;	$\beta_s^{-} = 0.983779 + 27.1 \times 10^{-6} C_s$	(16)
From average to good soil condition	$\beta_s^{+} = 1.006188 - 10.3 \times 10^{-6} C_s$;	$\beta_s^{+} = 1.008422 - 14.0 \times 10^{-6} C_s$	(17)

Modifier for Pipe Material, β_m

The modification of the loss algorithm for materials is based on the failure strain (measurement of ductility) of the material, ε_f. It is assumed that the slope of the algorithm in the semi-log axis will remain constant while the material property will shift the loss (damage) line horizontally, i.e. changing the constant term of the straight line. The modifier, β_m is for the pipe material defined as follows:

$$\beta_m = \frac{\epsilon_f}{0.003} \qquad (18)$$

The above equation is referenced to the failure strain $\varepsilon_f = 0.003$ of cast iron pipe.

Modifier for Continuous Pipeline, β_c

Since the referenced pipeline is a segmented pipeline, both the pipe strains and joint displacements are taking up the seismic ground strain. For pipelines without joints, pipe strain will be solely responsible to take up the seismic ground strain. The modifier, β_c will be:

$$\beta_c = \frac{\epsilon_f}{0.003 + \frac{2.5}{600}} = \frac{\epsilon_f}{0.00717} \qquad (19)$$

Note that the above modifier resumes a 2.5 cm joint movement capacity over a 6m pipe segment length.

Modifier for Joint Construction, β_j

The modifier for joint construction β_j, will be based on the ultimate joint displacement, Δ_f with reference to the ultimate joint displacement of a rubber gasket joint in a 12" (30 cm) pipe.

$$\beta_j = \frac{\Delta_f\,(\mathrm{cm})}{2.5} \qquad (20)$$

Modifier for Year of Construction, β_y

It is assumed that the failure or damage of pipeline will be 50% or more for pre-1950 construction and 50% or less for post-1950 construction. Therefore,

$$\beta_y^- = 1/2 \qquad \text{and} \qquad \beta_y^+ = 2 \tag{21}$$

Please note that the above modifier is adopted for demonstration purpose. More statistical analysis on damaged pipes would be needed to give better correlation.

GIS APPLICATIONS

INTRODUCTION

Geographic Information System (GIS) is a computer-based multi-functional tool for integrating, analyzing and managing geographically referenced data from many sources. Today's GIS technology has the capability to store sizable network maps into an indexed spatial database which is based on the topological structure of network segments. Simultaneously each network-segment's features are stored into a GIS's attribute database. By using GIS's inquiry functions, a potential liquefaction zone can be overlaid on water and sewer networks and displayed on a computer monitor window. Within the zonal boundary, each pipeline's features can be posted on the screen and can also be statistically summarized into a report.

GIS has several major contributions to this project. First, it creates a more efficient way to derive the earthquake loss estimation for pipelines than the current method in practice. The developed model has proved to be faster in figuring out the replacement cost, since all the processing steps are automated and streamlined. The current practice is still in semi-automated manner. Second, the model can more accurately and flexibly depict the features of individual pipelines than the existing method which groups pipeline features within a grid overlay. In addition, the model can help a city conduct the pre-earthquake planning by identifying the potential weak spots on the network. And finally, during the earthquake, the model can help speed up repair works and set up priorities based on the importance to the network operations and the size of the affected area.

The overall general process for the model development is, first, to combine areawide maps of soil and seismic conditions to produce the map of potential liquefaction zones by rank; second, to use each liquefaction potential zonal boundary as a spatial limit to retrieve the specified pipelines within the zone onto a graphic screen and simultaneously to generate a file containing each displayed pipeline's length, material and diameter; and finally, to multiply the pipeline length by a pipeline failure rate and by a pipeline replacement cost per unit length to obtain the total loss-estimation of the system.

INVENTORY SCOPE.

Figure 6, which is the common factors map, shows the overall study area and the two specific drainage basins; Fiske and Tanner, in the city of Portland, Oregon. The spatial data are inventoried for the overall study area and more detailed for the two basins. The entire area, approximately 105 square miles, (270 square kilometers), contains the major portion of the Portland water and sewer systems. Aggregated parcels, water and sewer networks inventoried for Fiske and Tanner basins are about 2 and 2.5 square miles (5.1 and 5.9 km^2), respectively.

Large concentrated facilities have been inventoried over the entire area. The pipeline joints are inventoried within two drainage basins.

One of these tested areas (Tanner) contains critical water transmission and storage facilities and sewage collection facilities serving a portion of the central business district of downtown Portland. The other basin (Fiske) includes the principal sewage treatment plant for the city of Portland, the Columbia Boulevard Sewage Treatment Plant.

DATA ORGANIZATION

The organization of spatial data in accordance with the GIS general principles concerns about the linkage between a graphic and its associated attribute databases, the dynamic retrieval from databases, and the elimination of data duplications in storage. These principles are carried out for inventorying different types of data for this project.

For example, the soil liquefaction potential map contains several source information, which can be retrieved in whole or in parts. The soil liquefaction potential map is derived from the combination of two maps, namely, the seismic intensity and surface soil liquefaction susceptibility maps. On the soil liquefaction potential map, there are major highway networks and the boundaries of selected basins. Both of them are retrieved from the common factors map, which eliminates the duplications of data elements and assures the data integrity among various functional maps.

The common factors map, first, contains the concentrated facilities distinguished by function associated with their major attributes which are stored into the non-spatial database. Second, it has a layer of major water transmission lines linking the source reservoir with subsequent reservoirs, pumping stations, and tanks. Third, for a clarity in orientation, it has the regions major highway network and large water bodies. Fourth, it also indicates the selected basin areas for detailed pipeline inventories. And finally, it contains a map's basic components such as map legend, north arrow sign, scale ruler and border. All of the above common factors can be totally or partially overlaid onto a functional map. The common factors map will not only enhance a map's legibility and also improve the coherent appearance and consistency among maps.

Prior to the data entry, all the data items are listed and defined in a data dictionary as summarized in table 1 for spatial and non-spatial databases.

TABLE 1
Summary Of Database Dictionary

DATA TYPE	COMPONENT	SPATIAL DATABASE	ATTRIBUTE DATABASE
Soil Seismic Geology	zone	layer name hatch pattern line types	zonal ID
Water Node	valve, joint	valve symbol joint symbol	device ID
Water Pipe	pipe segment	layer name features	segment ID diameter material length year installed
Sewer Node	manhole	symbol	device ID
Sewer Pipe	pipe segment	layer name features	segment ID diameter material length
Parcel	parcel	layer name features	parcel ID parcel area

INVENTORY SOURCES

The spatial data sources used for this project are not in the computerized format. Most are data on paper maps. Some of the data are available on computer tapes. The size of the data file, however, covers a much larger region than this project scope. The load and the generation of the original source map impose difficulty onto the PC and workstation with their limited memory size and processing speed.

Two major types of maps were used for this project. The first type is USGS Portland area quadrangles, 7.5 minute series topographic maps with soil and rock data from the Oregon Department of Geology and Mineral Industries. The second type is maps from the Portland City Bureau of Water Works water and sewer networks, containing their attributes, and parcel information.

INVENTORY TOOLS

Software

Two GIS software packages are used for this project because of their relatively low cost and applicabilities. One is the Facility Mapping System for AutoCAD (FMS/AC) (1989) purchased from Facility Mapping System, Inc. in Mill Valley, California. Another is Geo/SQL (Generation 5 Technology, Inc., 1989) granted from Generation 5 Technology, Inc. in Denver, Colorado.

For illustrative and comparative purposes, FMS/AC is used for the inventory of the Tanner drainage basin, and Geo/SQL for Fiske in Portland City.

Both software packages use AutoCAD as a drawing engine. Both packages have the capability to link to a user selected Relational Database Management System (RDBMS) for managing attributes or texture data. Each software, however, has its original RDMBS. FMS/AC uses dBase III Plus. While the Geo/SQL uses R:Base. This project has used their original RDBMS's.

The major differences for the two GIS softwares are that FMS/AC adopts the AutoCAD's methodology to manage the graphic data while Geo/SQL creates its own spatial database. The Geo/SQL spatial database approach can ensure more on graphic data integrity and can generate a user specified portion of a map instead of the whole map as FMS/AC does. Consequently, Geo/SQL can handle a larger-sized project with ease, Geo/SQL has expedited this project operation.

Due to the difference of the spatial data base structures between the two softwares, the data retrieval capabilities are also different. FMS/AC has the water and sewer network tracing capabilities in case of pipeline breakages. Thus, the affected pipelines can be automatically illustrated on the screen. This functionality, however, didn't perform up to this project's requirements. Geo/SQL can inquire the attribute data by graphically defining the area in a free shaped polygon.

In the Geo/SQL environment, the area directly served by the water or sewer pipeline can be graphically defined by using the polygon retrieval feature. All the parcels within the operator-defined polygon can be retrieved from the attribute database for tabulation and statistics. The codings of water and sewer segments IDs on a parcel record are not necessary under the Geo/SQL environment.

LOTUS is used at the last stage of the modeling for the calculating and generating the tabulated report on the replacement cost for those damaged pipelines.

In short, a set of four types of softwares are required, i.e. AutoCAD, GIS, RDBMS, and LOTUS.

All of the above mentioned softwares operate in the DOS environment in version 3.2. They are also installed in the DOS and UNIX environments on a Sun workstation.

Hardware

Both FMS/AC and Geo/SQL software packages can be operated on an IBM compatible 286 PC. All the project required functionalities from Geo/SQL can work on a Sun workstation 386i.

This project has used both PC and Sun workstation 386i for demonstration purposes for two drainage basins.

The PC used for this project contains 3.2 megabytes of RAM and a hard disk of 30 megabytes. The 386i has 8 megabytes of RAM and 91 megabytes of hard disk space.

The peripheral devices include a digitizing tablet with the size of 12" by 12" purchased from CalComp, an E-sized plotter with the manufacturing classification named DraftPro made by Hewlett Packard and one dot-matrix printer, Epson LQ-2500, connected to PC or Sun workstation by switching plugs.

INVENTORY FOR SOIL AND SEISMIC MAPS

The soil and seismic data overlayed on the USGS 7.5 minutes topographic series maps are used as graphic data sources, which are digitized by using AutoCAD as a drawing tool. These maps are first stored as AutoCAD drawings. Then, they are transferred into Geo/SQL's spatial database and their associated major attributes into R:BASE.

The basic digitized maps include surface soil, seismic intensity under local earthquake scenario, and seismic intensity under subduction earthquake scenario maps. By overlaying a seismic intensity map onto the surface soil map, the soil liquefaction potential map is generated. These maps will be presented and explained in later sections.

INVENTORY OF TANNER DRAINAGE BASIN BY FMS/AC

Prior to the data inventory, the entire Tanner drainage basin area is divided into three parts. Each part has approximately 300 to 350 parcels. The divisions will reduce the drawing generation time in the AutoCAD environment. The FMS/AC's large file management module can merge all the parts together. However, this merging was very time consuming on our PC.

Parcel Inventory

The definition of parcel here is a group of lots directly served by one water pipeline segment. Often one city block represents one or two parcels.

FMS/AC provides the functionality for parcel attribute data entries after the parcel map is digitized into the AutoCAD environment. Each parcel ID and area are entered from the keyboard and posted as an AutoCAD attribute block within the parcel at the insertion point entered by the operator.

A parcel size can be derived from the AutoCAD function for an area calculation. A parcel ID is derived from the city's existing system. A parcel ID is a 7-digit number obtained (1) by combining the city's quad sheet number, which is given in 4-digits; (2) within the quad, block numbers are assigned with 2-digits; and (3) within the block, each parcel is assigned 1-digit. An example is 2025-10-1, which represents quad sheet number 2025, block number 10 and parcel number 1.

For the purpose of identifying the affected area, once a pipeline breakage occurs, the ID of a pipeline segment directly connected to a parcel is coded onto the parcel's attribute block, which therefore contains 4 data items: parcel ID, parcel size in square feet, water pipeline segment ID, and sewer pipeline segment ID. In addition, there are two more data items, handle number, and insertion point coordinates (x, y) on a parcel record. The latter two data items are entered automatically. The AutoCAD handle number here is used as a linkage between a parcel drawing entity and a parcel's attribute record in the RDBMS.

By using the AutoCAD extract-attribute function, each parcel's attributes posted on the parcel map can be extracted from the drawing and written into a sequential ASCII file. And subsequently, this texture file can be loaded into the dBASE III Plus database.

Figure 7 shows the Tanner drainage basin parcel database.

Network Inventory

After the parcel map is prepared, it serves as a locational reference for entering water and sewer devices and pipelines.

There are many similarities between water and sewer network data inventories. The only difference is that a sewer pipeline segment ID is defined by the sewage flow direction.

Prior to the entry of the water network data, the water network is divided into segments. Each segment is defined by two end joints which can be a valve or other type of device. Each pipe joint needs an unique ID which has to be assigned.

On the city's water quad map, a majority of joints have already been assigned IDs by the city. A pipe joint is often a water valve (the symbol, '8', represents a water valve) which can be opened and closed to control water flow or a pipe connector (the symbol, 'o', represents a connector) not having the feature to shut off the water flow. All the city-assigned joint IDs have been kept intact and integrated into the project. In addition, some joints are added and new IDs are assigned. The new IDs are a continuation of the existing number series.

For establishing the water network coding standards, the rules for assigning a joint ID are illustrated and explained in table 2:

A water pipeline's ID is a combination of two end joint IDs. For consistency and later data retrieval from dBASE III Plus, a pipeline's ID is formed by having a smaller joint ID value placed first and a larger joint ID value following, such as 202513-202513a or 202513a-202514. A sewer pipeline's ID is also a combination of two end joints IDs. According to the sewage flow direction, the from- end ID is placed first and the to-end ID follows.

Both water and sewer pipe attributes include four data items which are pipe ID, diameter, material, and length. The length has been automatically calculated by the system instead of input by the operator. Those data items are entered whenever they are available and verified by the city of Portland.

Figure 8 shows the Tanner Drainage Basin Water Network Database and figure 9, the Tanner Sewer Network Database.

TABLE 2
Network Joint ID Coding Rules

SYMBOL	DESCRIPTION
-----o----- -----8-----	Two pipes with a standing alone joint. The joint ID is a 6 digit number. The first 4 digits represents the city's water quad sheet number. The following 2 digits represent the city assigned joint series number on that quad. For example, a joint number can be 202512.
I 8 a 12 I -----o--8-- b	Three pipes with an open join and two valves. For example: the open joint "o" ID is 202512; first adjacent valve "8" ID is 202512a; second adjacent valve "8" ID is 202512b.
I 8 a 13 I -----o--8--- I b 8 c I	Four pipes with an open joint and three valves. For example: the open joint "o" ID is 202513; first adjacent valve "8" ID is 202513a; second adjacent valve "8" ID is 202513b; third adjacent valve "8" ID is 202513c.
I I13 13a o-----8 I I I I -----I-----o-----8----- I 14 14a I	Two long pipes jointed by a short pipe near the intersection, each joint has its ID such as 202513 and 202514; its adjacent valve ID then as 202513a and 202514a respectively.

NOTE: Symbol 'o' represents an open connector, '8' represents an open-and-close connector such as a valve)

INVENTORY OF FISKE DRAINAGE BASIN BY Geo/SQL

Database Preparation

Prior to the data entry, a spatial database needs to be created. The Geo/SQL's spatial database divides the entire mapping area into sub-units, called grids. A map's features are stored by grid identifications. Grids serve as index units for a direct access to a grid containing those search features. Therefore, a grid size should not be too large to prolong the search time. But if the grid is too small, the index file will be large, which in turn increases the overhead time. There is a need to optimize the grid size.

Two other factors are needed to be specified during the creation of a partial database. The first factor approximates the center location of the mapping area. The second factor sets the tolerance level. This specification allows the snap of two nearby points together for eliminating duplicated incidental lines if they are within the tolerance level.

The grid size for this project is 1000 feet by 1000 feet. The center of the mapping area is 31,680 feet for x-coordinate and 31,680 feet for y-coordinate measured from the lower left corner of the map. The tolerance level is 1 foot. The database is further divided into subjects. For this basin, the database includes subjects of 'watpipe', 'watnode', 'sewpipe', 'sewnode', and 'parcel'.

Parcel Inventory

Geo/SQL identifies a parcel as a polygon. Once an AutoCAD drawing of parcels has been created, each parcel has to go through a polygon integrity checking process with an operator- specified polygon tolerance level for accepting an imperfectly conditioned polygon with a gap between two end joints. The next step is to insert a unique polygon ID, which is a parcel's ID, stored in R:BASE. Those attribute data were in dBASE III Plus. They were transferred from dBASE III Plus into R:BASE by using the R:BASE utility.

After each polygon has been assigned with a unique ID at the inserted point called Designated Interior Point (DIP), an indexed file is automatically created containing a list of all DIPs for the polygons. Then the polygons are ready to be loaded into the Geo/SQL's spatial database under the subject named 'parcel'.

During the loading process, each polygon is assigned a unique object number, which is also assigned to its corresponding attribute data record in R:BASE. The object number serves as a link between an object in Geo/SQL's spatial database, such as a parcel polygon, and its attribute data record in R:BASE.

After the AutoCAD drawing is stored into the spatial database, the drawing can be erased from the AutoCAD drawing file. By using Geo/SQL's inquiry capability, the parcel map and its attributes can be retrieved from databases in a user-specified condition. Figure 10 shows the Fiske Drainage Basin Parcel Map, retrieved from two databases. The map represents the contents of the databases.

Network Inventory

Geo/SQL considers pipelines as line or arc objects and manholes, valves and joints as point objects. All the AutoCAD line works should be drawn by line or arc option. By using Geo/SQL's fracturing and exploding functions, an AutoCAD drawing can be converted and complied with the Geo/SQL's drawing requirements.

To inventory the network, the first task is to convert each pipeline's attribute data by transferring them from dBASE III Plus to the 'watpipe' and 'sewpipe' tables respectively in R:BASE. The attribute record contains pipeline ID, material, diameter, and length. The 'watpipe' table has one additional data item which is the year of installment of a pipeline segment.

The next step is to insert each pipeline segment ID from the table in R:BASE onto the associated pipeline segment. For this operation, a group of pipeline IDs is selected from R:BASE. Subsequently each selected pipeline ID appears on the menu screen to be posted onto the corresponding pipeline displayed on the AutoCAD screen.

After assigning unique IDs to pipelines, the pipelines can be loaded into the spatial database under the subject named 'watpipe' or 'sewpipe' respectively. During the loading process, an object number is assigned to each water pipeline or sewer pipeline. That object number will also be assigned to the associated pipeline record within the 'watpipe' or 'sewpipe' table in R:BASE.

As for devices, valves, joints and manholes are point objects. The data entering and loading processes for line or point objects are the same, since they are both classified by Geo/SQL as simple objects when polygons are complex objects.

After a network is transferred into a spatial database and its attributes in R:BASE, the AutoCAD drawing for water or sewer can be erased from the hard disk. Using the Geo/SQL inquiry capabilities, a user can flexibly retrieve the map and texture data.

Figures 11 and 12 show the Fiske drainage basin water and sewer networks retrieved from the databases.

SEISMICITY IN PORTLAND, OREGON

To estimate the seismic damage of Portland water and sewer systems, two earthquake scenarios have been adopted and studied. One highly probable scenario is the Local Earthquake Scenario (LES) in which an earthquake of a magnitude M = 6.5 occurs directly under Portland. Another less probable scenario is the Subduction Earthquake

Scenario (SES) in which a large earthquake of M = 8.4 occurs at the Pacific coast far away from Portland. The study of these two scenarios is for demonstration purposes and does not represent an attempt to rigorously predict earthquake shaking or damage. The characteristics of these two earthquake scenarios are described in the following subsections:

LOCAL EARTHQUAKE SCENARIO (LES)

The seismicity of the Portland area under LES was studied based on previous publications by Cornforth (1986), and Couch and Peterson (1971). The most probable earthquake seismicity at the area was chosen as M = 6.5 and the maximum peak ground acceleration of 0.32g.

The other possible earthquake sources may be from the Puget Sound, Washington region. Cornforth's study (1986) showed that the potential earthquake source in the Puget Sound region contributes little to the hazard at the site, so the local earthquake source is selected for this Portland area study.

Based on the selected earthquake source, a seismic response map of the Portland area for the LES can be generated. Although the possible source zone has not been pinpointed, Couch and Peterson (1971) obtained a seismic response map of the Portland area for local earthquakes, which is used for demonstration purposes only. The maximum intensity area (+2.5 to +3.5 over expected intensity) as MMI = IX area with the peak ground acceleration of 0.32 g was assigned. The lower intensity areas follow accordingly as listed in table 3:

In Table 3, the relationships between intensity and peak ground acceleration are according to Okamoto's general relations (1984) as seen in Figure 13. The curve selected for Portland lies within Okamoto's range. Note that the peak ground acceleration 0.32 g was reported in a seismicity study by Cornforth (1986) for Mt. Tabor area in Portland but as interpreted that value is for the general Portland area.

TABLE 3
Relationships Among Intensity Anomaly Key and Earthquake Intensity, and Peak Ground Acceleration Under 'LES'

Intensity Anomaly Key*	Earthquake Intensity (MMI)	Peak Ground Acceleration
+2.5 - +3.5	IX	0.32 g
+1.5 - +2.5	VIII	0.21 g
+0.5 - +1.5	VII	0.12 g
-0.5 - +0.5	VI	0.07 g
-1.5 - -0.5	V	0.03 g
-2.5 - -1.5	IV	0.0 g

This intensity map has been inventoried into the GIS database. Figure 14 shows the intensity map for the Portland area under LES. Figure 15 shows the map superimposed onto the Fiske Sewer Network with the seismic intensities in a larger scale retrieved from the GIS inventory.

SUBDUCTION EARTHQUAKE SCENARIO (SES)

Although a larger subduction earthquake is less likely to occur than smaller local earthquakes in Portland, Madin (1989) outlines the earthquake hazards in Portland in a recent paper. According to Madin's opinion, an earthquake of M = 8.4 at the Cascadia Subduction Zone 75 km away from Portland may be possible. For demonstration purposes, the Subduction Earthquake Scenario (SES) is also considered here.

Using the attenuation curve developed by Seed and Idriss (1982), the peak ground acceleration at the rock site would be 0.18 g for a distance of 75 km. The intensity in MMI scale would be between VII and VIII on bedrock. However, it should be recognized that this intensity may not give a true indication of damage, because the long duration (60 seconds or more) of the subduction zone earthquakes is not taken into account.

Based on the selection of the SES, the seismic response map of the Portland area for distant earthquakes is developed. Figure 5 of the Couch and Peterson Report (1971) shows the intensity anomalies obtained in the Portland area for distant earthquakes. A zero anomaly zone as VII - VIII intensity with 0.18 g was assigned. Accordingly the

***In fig. 4 of Couch and Peterson's report (1986)**

minimum intensity area in the map (+0.5 to +1.5 over expected intensity) indicated as VIII area is assigned with the peak ground acceleration of 0.21 g. The higher intensity area will follow as listed in table 4.

In table 4, the relationships between intensity and peak ground acceleration are according to Okamoto's general value (1984). The curve selected for Portland lies within the Okamoto's range.

The seismic intensity map for Tanner drainage basin under SES was retrieved from the GIS database shown in figure 16.

TABLE 4
Relationships Among Intensity Anomaly Key, Earthquake Intensity and Peak Ground Acceleration Under 'SES'

Intensity Anomaly Key**	Earthquake Intensity (MMI)	Peak Ground Acceleration
0	VII - VIII	0.12 g
+0.5 - +1.5	VIII	0.21 g
+1.5 - +2.5	IX	0.32 g
+2.5 - +3.5	X	0.49 g
+3.5 - +4.5	XI	0.66 g
+4.5 - +5.5	XII	0.82 g

SOIL LIQUEFACTION POTENTIAL STUDY FOR PORTLAND

The liquefaction potential for the Portland, Oregon area during a future earthquake was assessed by following two steps: (1) preliminary assessment based on the area's surficial geology, and (2) detailed evaluation on individual boring logs based on the critical standard penetration values (N_{cr} values) using the available soil stratification and the ground water table information.

PRELIMINARY ASSESSMENT

The surficial geological map was divided into five liquefaction susceptibility categories, namely: (1) very high, (2) high, (3) moderate, (4) low, and (5) very low zones for liquefaction evaluation, based on the criteria provided

****In fig. 5 of Couch and Peterson's report (1986)**

by Youd and Perkins (1978). With the assistance of a project geologist, Ian P. Madin of Oregon Department of Geology and Mineral Industries, the following classifications were made for the area:

Geological symbols		Liquefaction Category
Q_{af}:	Artificial Fill	Low
Q_{al}:	Alluvium	High
Q_{fc}:	Coarse-grained Facies	Very Low
Q_{fch}:	Channel Facies	Very Low
Q_{ff}:	Fine-grained Facies	High
Q_{ls}:	Loess	High
All Others:		Very Low

Figure 17 shows the surficial soil liquefaction susceptibility of Portland. Note that this area has only three categories: high, low, and very low, without very high and moderate liquefaction susceptibilities.

The liquefaction potential map was created by overlaying two previously prepared maps: (1) liquefaction susceptibility map which was developed based on surficial geology, and (2) seismicity map which was obtained from historical intensity observations for a given earthquake scenario.

DETAILED EVALUATION ON INDIVIDUAL BORING LOGS

Detailed liquefaction potential evaluations have been conducted for areas where the liquefaction susceptibility is higher than the moderate category. Available boring logs have been investigated on their water table elevation, soil type, and standard penetration values (N values).

If the water table elevation is lower than 33 feet, no further analysis is needed since buried pipes near the ground surface would not be affected by the deep zone liquefaction unless lateral spreading occurs. Analysis of susceptibility to lateral spreading is beyond the scope of this study. When the water table elevation was not reported, it was assumed to be at the ground surface as a conservative assumption.

Only soil deposits under the water table have been assessed for liquefaction potential. Sand and silty soils are considered liquefiable while gravelly, clayey, and organic soils are non-liquefiable. Then, the critical N-value for liquefaction was established for each ground water table elevation according to Seed and Idriss criterion (1982), and compared with the measured field N-value for the detailed liquefaction evaluation.

LIQUEFACTION POTENTIAL MAP UNDER 'LES' (M = 6.5)

As discussed earlier, a soil liquefaction susceptibility map normally employs five (5) categories, according to Youd and Perkins' ranking (1978). For the Portland area, however, its highest category is 'high' so that it reduces to four categories. On the other hand, the seismic intensity map (fig. 14) has 6 categories from 0.32g, 0.21g, 0.12g, 0.07g, 0.03g, to 0.00g for the 'LES' of M = 6.5 earthquake. The combination of these two maps creates a total of 24 possible ranks (4 x 6) in terms of the liquefaction potential. Based on the engineering judgment and the comparison with the detailed liquefaction evaluation, liquefaction potential ranks have been assigned as "very high", "high", "medium high", "medium", "low", and "very low" as indicated in table 5.

It is noted that "poor soil" will be corresponding to "high" liquefaction susceptibility, "average soil" to "medium" and "good soil" to "low" and "very low" liquefaction susceptibility. It shall also be noted in the table that a "low liquefaction potential" rank was assigned for 0.32g seismicity at a very low liquefaction susceptibility block. This is because even under a very high acceleration, the area will not liquefy if the soil is not liquefiable.

The liquefaction potential map retrieved under LES from the inventory database is shown in figure 18.

For only (1) very high, (2) high, and (3) moderate liquefaction potential zones in figure 18, available boring logs were investigated by comparing the critical N-value and its field N-value of a liquefiable soil type. The engineering judgment was made for each boring log for high, moderate, or low liquefaction potential. The results of detailed liquefaction potential analysis of available boring logs under LES are shown in figure 19.

TABLE 5
Liquefaction Potential Ranks Under "LES"

Peak Ground Acceleration	Liquefaction Susceptibility			
	High (Poor Soil)	Medium (Average Soil)	Low (Good Soil)	Very Low (Excellent Soil)
0.32 g	very high	high	medium high	low
0.21 g	high	medium high	medium	low
0.12 g	medium high	medium	low	very low
0.07 g	medium	low	very low	very low
0.03 g	low	very low	very low	very low
0.00 g	very low	very low	very low	very low

* Note that non-liquefiable soil may be considered as Excellent Soil.

When the detailed liquefaction study with limited boring logs is compared with the liquefaction potential map (fig. 18), those categories generally agree with each other. However, due to the locality of soil conditions, it is impossible to obtain a one-to-one match. Therefore, figure 18 should be used only for a preliminary assessment of the liquefaction potential. For an important building or structure, new borings at the site or at least nearby boring logs should be used to carry out a detailed analysis for such a project.

LIQUEFACTION POTENTIAL MAP UNDER SES (M = 8.4)

As indicated earlier, the normal liquefaction susceptibility map originally has five categories, but in the Portland area, its highest category was high. Under SES, the seismic intensity map has 6 categories varying from 0.82g, 0.66g, 0.49g, 0.32g, 0.21g, to 0.12g for the M = 8.4 earthquake. The combination of two maps creates total 24 possible ranks (4 x 6) in terms of liquefaction potential. Again, based on the engineering judgment and the comparison with the liquefaction susceptibility map (fig. 17), the following liquefaction potential ranks were assigned as shown in table 6:

The above liquefaction potential ranking is compatible to the ones assigned in the LES analysis. It also shall be noted that all blocks in "very low" liquefaction susceptibility column are assigned to have "low" potentials since it is not likely to liquefy even with a high acceleration for non-liquefiable soils.

Four selected boring logs were further studied for detailed liquefaction analysis. These have been evaluated to have a low to medium liquefaction potential under LES. Under this earthquake scenario (SES) these four sites are all classified as "high" liquefaction potential due to extremely high acceleration levels.

TABLE 6
Liquefaction Potential Ranks Under "SES"

Peak Ground Acceleration	**Liquefaction Susceptibility**			
	High (Poor Soil)	**Medium (Average Soil)**	**Low (Good Soil)**	**Very Low (Excellent Soil)***
0.82g	very high	very high	very high	low
0.66g	very high	very high	very high	low
0.49g	very high	very high	high	low
0.32g	very high	high	medium high	low
0.21g	high	medium high	medium	low
0.12g	high	medium high	medium	low

* Note that non-liquefiable soil may be considered as Excellent Soil

Retrieving from the GIS database, the earthquake liquefaction potential map for Portland under SES is shown in figure 20.

LOSS ESTIMATION OF WATER AND SEWER PIPELINES

GENERAL DISCUSSIONS

The development of loss algorithms for buried pipelines under a seismic shaking environment has been presented earlier. The percent of total loss of buried pipelines (water and sewer) can be estimated for given soil conditions, pipe and joint materials, year of installation and earthquake intensity. There is no rigorous development to estimate a pipeline loss due to liquefaction. However, ATC-13 (Rojahn and Sharpe, 1985) recommends that under a soil liquefaction environment, asbestos cement (AC) pipe may have 4.5 breaks/km; Cast Iron (CI) pipe, 3 breaks/km; welded steel-caulked joint (WSCJ) pipe, 2.7 breaks/km, and welded steel welded joint (WSWJ) pipe may have 2.4 breaks without further details. If the 15 breaks/km limit is considered to be 10% loss, then 3% loss applies to AC pipe, 2% to CI pipe, 1.8% to WSCJ pipe, and 1.6% to WSWJ pipe under an average (medium) liquefaction potential condition. Adjustments should be made for high and low liquefaction potentials in order to take the severity of earthquakes into account. For simplicity and conservatism, the area with a "medium" liquefaction potential is considered to have an "average" soil condition, while the area with higher or lower than the "medium" liquefaction potential would be considered as having a "poor" or "good" soil condition discussed in the loss-algorithm model (figs. 2 to 4). Further refinement is out of the scope of this report.

FAILURE RATES OF BURIED PIPELINES

Although substantial efforts have been attempted to correlate earthquake damages to buried pipelines with various conditions, not enough field data has been found to justify further refinements other than the correlations between pipeline damages, materials, soil conditions, and earthquake MMI intensities.

As indicated earlier, three types of general soil conditions are considered, namely poor, average, and good soil conditions. These soil classifications can work with the soil liquefaction susceptibility classifications. Under "high" soil liquefaction susceptibility, the soil condition would be "poor". Similarly, the "medium" soil liquefaction susceptibility correlates to the "average" soil and the "low/very low" soil liquefaction susceptibility to the "good" soil condition.

Although numerous materials have been used for water and sewer pipelines, unfortunately, there is not enough damage data to make distinctions. Generally, one can classify a pipeline construction as brittle or ductile construction taking the materials and joints into account. The brittle construction includes cast iron (CI) pipe, concrete cylinder pipe (CCP), concrete sewer pipe (CSP), brick and stone (BS), vitrified sewer pipe (VSP), and asbestos (AC) pipe, etc. The ductile construction includes ductile iron (DI), steel (STL), reinforced concrete (RC), prestressed concrete (PC), and polyvinyl chlorine (PVC) pipes.

Using the information shown in the Development of a Loss Algorithm for Buried Pipelines Section, the following (table 7) failure rates are used as the demonstration of loss-estimation for Portland water and sewer pipelines.

TABLE 7
Failure Rate (percent) of Buried Pipelines

Earthquake Intensity		Brittle Construction			Ductile Construction		
MMI	g	Poor Soil	Average Soil	Good Soil	Poor Soil	Average Soil	Good Soil
XII	0.82	10%	10%	10%	10%	10%	10%
XI	0.66	10%	10%	10%	10%	10%	10%
X	0.49	10%	10%	10%	10%	10%	2.49%
IX	0.32	10%	10%	0.3%	10%	2.84%	0.07%
VIII	0.21	2.85%	0.02%	0.01%	0.71%	0.05%	0
VII	0.12	0.04%	0	0	0.01%	0	0
VI	0	0	0	0	0	0	0

UNIT REPLACEMENT COSTS

The unit replacement costs ($/ft) of water and sewer pipelines have been supplied by the City of Portland. It was based on U.S. Army Corps of Engineers, Engineering Manual EM 1110-2-507 November 1980 and Engineering News Record 4567, March 1989.

According to the 1989's price value, the replacement cost includes labor and materials for excavation, the replacement of a pipe of the same kind or better, and backfill.

Table 8 gives the unit replacement costs, U_r, for water pipelines and table 9 for sewer pipelines.

TABLE 8
Water Pipeline Unit Replacement Cost, U_t

Dia. (in.)	CI/DI ($/ft.)	STL ($/ft.)	CCP ($/ft.)
2	11	11	
4	22		
6	33		
8	44		
10	55		
12	66	66	
16	87	87	
18	97		
20	114	114	
24	150	140	
30	209		214
32	231		
36	275		285

TABLE 9
Sewer Pipeline Unit Replacement Cost, U_t

Dia. (in.)	CSP ($/ft.)	Mono CSP ($/ft.)	Brick Stone ($/ft.)	CI, PVC, VSP ($/ft)
6	60			60
8	70			70
9	80			80
10	90			90
12	100			100
14	110			110
15	115			115
16	115			115
18	130			130
20	140			140
21	145			145
24	160	160	295	160
27	195	195		195
30	230	230	362	230
36	295	295		295
38	318	318	452	318
42	365	365		365
48	430	430		430
54	495	495		
60		560		
66		630		
72		700	835	
78		770	902	
84		835		
90		905		
96		975		
102		1040		

Please note that in the subsequent calculations for demonstration purposes, linear interpolation from known costs will be used if the cost for a specific pipe is not available for the original supplies by the City of Portland.

TOTAL LOSS/REPLACEMENT COST ESTIMATION

Under an earthquake scenario, the earthquake intensity (MMI) and soil liquefaction susceptibility (soil condition) can be evaluated for a specific area or basin. The failure rate, γ_{ti}, of a specific type of pipeline construction for a given MMI can be obtained from table 7 or derived from loss estimation algorithm.

The inventories of total pipe length, L_t, for a specified type of pipeline material, diameter, joint etc. can be retrieved from the GIS system.

The total damaged length, l_{ti}, would be the product of the failure rate and the total length for a specific material and diameter pipe as:

$$l_{ti} = \gamma_{ti} \times L_t \tag{22}$$

Then the replacement cost for this specific pipeline would be the product of the damaged length by the unit replacement cost, U_t, obtained from table 8 or 9 as:

$$C_{ti} = U_t \times l_{ti} \tag{23}$$

The total loss/replacement cost of the network will be the sum of all types of pipe under all earthquake intensities in a study will be:

$$C_{total} = \sum_t \sum_i C_{ti} \tag{24}$$

MODEL OPERATION PROCEDURES FOR THE LOSS-ESTIMATION

There is more than one way to obtain the loss-estimation in pipelines. For an illustrative purpose, a common straight forward alternative is used here on an IBM AT micro-computer.

In general, under the menu driven guidance, even an inexperenced operator can utilize the system without difficulty. All the steps that an operator has to deal with are listed below:

A. In the DOS environment, when the PC power is on, select the AutoCAD option from a menu posted on the screen.
B. Select an edit drawing option from the AutoCAD main menu and enter the predefined prototype drawing name, "Portland", used for this project. That drawing is the base map for the Portland project.
C. Select the inquiry option from the Geo/SQL drop-down menu, and the user will be prompted with questions. The answers can be selected from the customized menu. The first set of questions is for locating the searched data items. The second set defines the conditions for retrieving the required data from the located data sources. And the third set determines the output formats in graphic and texture contents. Finally, the operator can use the listing option to display all of the specified conditions as shown in table 10.
D. Select the execution option from the inquiry menu to generate the entire pipeline system within a studied region (say high liquefaction potential region) on the screen. Simultaneously, a report file is generated.

TABLE 10
Inquiry Search List

Attribute Database:	Portlnd
Spatial Database:	Sportlnd
Table Name:	Watpipe
Subject Name:	Watpipe
Inquiry Type:	Objects
Graphic Format File:	highlique boundary
Selected Columns:	size, material, length
Geographic Search Criteria:	within Polygon

The inquiry file (table 10) can be saved and loaded into the menu. Then an operator only needs to select the inquiry from the menu, and load and execute the inquiry to get the result.

E. Type "RBASE" at the command prompt in the AutoCAD graphic environment. The R:BASE menu will subsequently appear for the operator to select the gateway's import option from the menu for importing the report file into R:BASE.
After the report file is in the table of R:BASE, it can be cross-tabulated and converted into a R:BASE table.

F. Select the gateway's export option from the R:BASE menu to transfer the cross tabulation of the pipelines' length by material and by size into the spreadsheet of LOTUS.
Once the data is in LOTUS, the pipelines' replacement costs can be easily calculated and displayed on a screen or printed on hard copy.
The total operation time for the above six steps for any replacement cost table is approximately 12 minutes in a 286 PC environment. If the inquiry file has been specified and stored, the total operation time will be under 10 minutes.
The operation procedures on SUN workstation is about the same, except a DOS window must be opened and under the DOSRUN condition, the retrieval time is approximately the same as on the PC.

DEMONSTRATION RESULTS

Preface

Using the developed model and procedures described in the previous sessions, the loss estimation or replacement costs of water and sewer pipelines in Fiske and Tanner Drainage Basins are given in the following subsections as demonstration results.

Due to limited man-power and resources, the accuracy in the inventory has not been thoroughly verified. Also, numerous assumptions and simplications have been used in soil classifications, loss algorithm, and earthquake scenario developments. The results shown are for demonstrating the connectivity and workability of the developed seismic loss estimation model and not for the actual implementation of an earthquake mitigation. However, with the additional support and effort, this model can be easily implemented as an actual earthquake hazard mitigation tool for any city or town that needs it.

In this study, two available GIS software packages, FMS/AC and Geo/SQL, have been used. It is found that Geo/SQL is relatively more convenient to use because of its spatial database structure. Therefore, a little more discussion will be given to the Geo/SQL system.

Fiske Drainage Basin

The data bases for the parcels, water and sewer networks of Fiske Drainage Basin have been shown in figures 10 to 12 respectively. Under the Local Earthquake Scenario, the earthquake intensity distribution can be seen in figure 14. Using the composite of figures, the sewer network versus MMI for Fiske Basin was shown in figure 15.

The surficial soil liquefaction susceptibility map, which describes the soil conditions, was shown in figure 17. One can see from figure 17 that a large portion of Fiske Basin is in the poor soil region (high soil liquefaction susceptibility), and a small portion in good soil region (low and very low soil liquefaction susceptibility).

By combining the earthquake intensity map (figure 14) and the surficial soil liquefaction susceptibility map (figure 17), the soil liquefaction potential map (figure 18) is obtained. The water and sewer networks within different liquefaction potential zones which signify the combined effects of soil conditions and earthquake intensities in Fiske are given in figures 21 and 22 respectively.

Figures 21 and 22 depict that Fiske has three different liquefaction potential regions. The high liquefaction potential region represents an intensity MMI = VIII within a poor soil condition. The medium high liquefaction potential region represents an intensity MMI = VII, and the medium region represents an MMI = VI. All three regions are within the poor soil condition as indicated in figure 17.

According to table 7, there will be no damage to buried pipelines for MMI = VI or less. This study will discuss the pipeline damages within high liquefaction (MMI = VIII) and medium high (MMI = VII) regions.

Extracted from the database, the lengths of various water pipelines of different diameters and materials under MMI = VII and VIII are given in tables 11 and 12. Similarly, the lengths of various sewer pipelines are given in tables 13 and 14.

Using the failure rate in table 7 and the unit replacement costs in tables 8 and 9, the estimated replacement costs for water pipelines under MMI = VII and VIII and the combination of the two are shown in table 15, 16, and 17 respectively. Similarly, the replacement costs for sewer pipelines are shown in tables 18, 19, and 20.

TABLE 11
Total Length of Water Pipelines in Fiske Drainage Basin
within Poor Soil an MMI = VII Region under LES

Dia. (in.)	CCP (ft.)	CI (ft.)	DI (ft.)	STL (ft.)	Total (ft.)
2				941.89	941.89
6		7181.10	2912.43		10093.53
8		9988.66			9988.66
12		3765.81			3765.81
36	1539				1539.00
Total	1539	20935.57	2912.43	941.89	26328.89

TABLE 12
Total Length of Water Pipelines in Fiske Drainage Basin
within Poor Soil and MMI = VIII Region under LES

Dia. (in.)	CCP (ft.)	CI (ft.)	DI (ft.)	STL (ft.)	Total (ft.)
2		304.93		1676.67	1981.60
4		914.69	1085.63		2000.32
6		10830.01	3953.16		14783.17
8		28927.87	648.58		29576.45
12		11589.67			11589.67
20				3865	3865.00
36	6770.22				6770.22
Total	6770.22	52567.17	5687.37	5541.67	70566.43

TABLE 13
Total Length of Sewer Pipelines in Fiske Drainage Basin within Poor Soil and MMI = VII Region under LES

Dia. (in.)	CSP (ft.)	MONOCSP (ft.)	VSP (ft.)	Total (ft.)
6	366.0		127.0	493.0
8	6218.1		3147.0	9365.1
10	1350.6		399.6	1750.2
12	1806.4		923.5	2729.9
15	2536.0		818.8	3354.8
18	276.5			276.5
24	735.5		1145.1	1880.6
72		779.8		779.8
Total	13289.1	779.8	6561.0	20629.9

TABLE 14
Total Length of Sewer Pipelines in Fiske Drainage Basin within Poor Soil and MMI = VIII Region under LES

Dia. (in.)	CSP (ft.)	MONOCSP (ft.)	VSP (ft.)	Total (ft.)
6	1020.9		205.0	1225.9
8	16213.9		4607.9	20821.8
10	4186.4		1773.7	5960.1
12	8703.1		1294.6	9997.7
15	8124.5		818.8	8943.3
18	2208.7			2208.7
21	220.9		609.8	830.7
24	2147.2		1448.2	3595.4
30	439.7	3215.7		3655.4
36		1370.8		1370.8
42		419.8		419.8
72		3493.0		3493.0
Total	43265.3	8499.3	10758.0	62552.6

TABLE 15
Water Pipeline Replacement Estimates in Fiske Basin within Poor Soil and MMI = VII Region under LES

Dia. (in.)	CCP $	CI $	DI $	STL $	Total $
2				1.04	1.04
6		94.79	9.61		104.40
8		175.80			175.80
12		99.42			99.42
36	175.45				175.45
Total	$175.45	$370.01	$9.61	$1.04	$556.10

TABLE 16

Water Pipeline Replacement Estimates in Fiske Basin
within Poor Soil and MMI = VIII Region under LES

Dia. (in.)	CCP $	CI $	DI $	STL $	Total $
2		95.60		130.95	226.54
4		573.51	169.58		743.09
6		10185.62	926.23		11111.85
8		36275.55	202.62		36478.17
12		21800.17			21800.17
20				3128.33	3128.33
36	54991.11				54991.11
Total	$54,991.11	$68,930.45	$1,298.42	$3,259.28	$128,479.26

TABLE 17

Water Pipeline Replacement Estimates in Fiske Basin
within Poor Soil and MMI = VII & VIII Regions under LES

Dia. (in.)	CCP $	CI $	DI $	STL $	Total $
2		95.80		131.98	227.58
4		573.51	169.58		743.09
6		10280.41	935.84		11216.25
8		36451.35	202.62		36653.97
12		21899.59			21899.59
20				3128.33	3128.33
36	55166.56				55166.56
Total	$55,166.56	$69,300.46	$1,308.03	$3,260.32	$129,035.36

Under Local Earthquake Scenario the total estimate for replacement costs is approximately $130,000 for the water pipeline (Table 17) and $255,000 for the sewer system (Table 20). This indicates that the damage of large sewer pipes will be more costly. It also indicates that pipelines in intensity MMI = VIII are damaged much more than that in MMI = VII region.

Tanner Drainage Basin

For the study of loss estimation/replacement costs in Tanner Drainage Basin, the Subduction Earthquake Scenario (SES) was used. Under SES, Tanner would be in the earthquake intensities MMI = XI. The damage to all pipelines will reach their maximum failure rate, i.e. 10%.

Without further discussions and explanations, the results of the study for Tanner Drainage Basin are given in the following figures and tables:

- FIGURE 23 Tanner Drainage Basin Water Pipes Damage Potential within Various Liquefaction Potential Zones under SES

- FIGURE 24 Tanner Drainage Basin Sewer Pipes Damage Potential within Various Liquefaction Potential Zones under SES

- TABLES 21, 22 Total Length of Water Pipelines in Tanner Drainage Basin within Good and Poor Soil Conditions and MMI = XI Region under SES

TABLE 18
Sewer Pipeline Replacement Estimates in Fiske Basin
within Poor Soil and MMI = VII Region under LES

Dia. (in.)	CSP $	MONOCSP $	VSP $	Total $
6	8.78		3.05	11.83
8	174.11		88.12	262.22
10	48.62		14.39	63.01
12	72.26		36.94	109.20
15	116.66		37.66	154.32
18	14.38			14.38
24	47.07		73.29	120.36
72	0.00	218.34		218.34
Total	$481.87	$218.34	$253.44	$953.66

TABLE 19
Sewer Pipeline Replacement Estimates in Fiske Basin
within Poor Soil and MMI = VIII Region under LES

Dia. (in.)	CSP $	MONOCSP $	VSP $	Total $
6	1745.74		350.55	2096.29
8	32346.73		9192.76	41539.49
10	10738.12		4549.54	15287.66
12	24803.84		3689.61	28493.45
15	26628.05		2683.62	39311.67
18	8183.23			8183.23
21	912.87		2520.00	3432.87
24	9791.23		6603.79	16395.02
30	2882.23	21078.91		23961.15
36		11525.00		11525.00
42		4366.97		4366.97
72		69685.35		69685.35
Total	$118,032.04	$106,656.23	$29,589.87	$254,278.15

TABLE 20
Sewer Pipeline Replacement Estimates in Fiske Basin within Poor Soil and MMI = VII & VIII Regions under LES

Dia. (in.)	CSP $	MONOCSP $	VSP $	Total $
6	1754.52		353.60	2108.12
8	32520.84		9280.88	41801.71
10	10786.74		4563.93	15350.66
12	24876.09		3726.55	28602.64
15	26744.70		2721.28	29465.99
18	8197.61			8197.61
21	912.87		2520.00	3432.87
24	9838.30		6677.08	16515.38
30	2882.23	21078.91		23961.15
36		11525.00		11525.00
42		4366.97		4366.97
72		69903.69		69903.69
Total	$118,513.91	$106,874.57	$29,843.32	$255,231.80

TABLE 21
Total Length of Water Pipelines in Tanner Basin within Good Soil and MMI = XI Region under SES

Dia. (in.)	CI (ft.)	DI (ft.)	STL (ft.)	Total (ft.)
2	2480.1	3745.1		6225.2
4	1620.9	1777.0		3397.9
6	13423.3	5622.4		19045.7
8	4449.5	25.1		4474.6
10	1095.3			1095.3
12	1673.9	1148.0	636.1	3458.0
16		218.0		218.0
Total	24743.0	12535.6	636.1	37914.7

TABLE 22
Total Length of Water Pipelines in Tanner Drainage Basin within Poor Soil and MMI = XI Region under SES

Dia. (in.)	CI (ft.)	DI (ft.)	STL (ft.)	Total (ft.)
2	6170.6	2283.1	2336.5	10790.2
4	8646.6	1445.7		10092.3
6	69388.1	3335.4		72723.5
8	56486.9	3659.8		60146.7
10	17929.7			17929.7
12	24785.8	1446.7	455.5	26688.0
16	2781.4		793.3	3574.7
18	382.3			382.3
20	9966.5			9966.5
24	2016.6	1228.0	2363.0	5607.6
30	7378.1			7378.1
32	1437.0			1437.0
36	3577.3			3577.3
Total	210946.9	13398.7	5948.3	230293.9

- TABLES 23, 24 Total Length of Sewer Pipelines in Tanner Drainage Basin within Good and Poor Soil Conditions and MMI = XI Region under SES

- TALBES 25, 26, 27 Water Pipeline Replacement Estimates in Tanner Drainage Basin within Good, Poor, and Combined Soil Conditions and MMI = XI Region under SES

- TABLES 28, 29, 30 Sewer Pipeline Replacement Estimates in Tanner Drainage Basin within Good, Poor, and Combined Soil Conditions and MMI = XI, Region under SES.

EARTHQUAKE HAZARD MITIGATION APPLICATIONS

APPLICATIONS TO PRE-EARTHQUAKE PREPAREDNESS

Within a high liquefaction area, the model can retrieve those pipelines most vulnerable to hazardous earthquake. Figure 25 illustrates some sizable pipelines installed half a century ago using the poor earthquake resistant material. They represent weak spots on the network in need of attention.

The model can also generate the report about those pipelines in detail which will help plan improvement strategies.

APPLICATIONS TO POST-EARTHQUAKE EMERGENCY RESPONSES

After a hazardous earthquake, a reported location with problems can be investigated by using the model. Figure 26 illustrates the retrieval of pipelines and parcel information within a radius of 750 feet from each reported site. A pipeline's attributes can be posted on the map and generated in reports. Such information will help figure out the repair process. By comparing the conditions of reported problem areas, a priority list for emergency responses can be established.

TABLE 23
Total Length of Sewer Pipelines in Tanner Drainage Basin within Good Soil and MMI = XI Region under SES

Dia. (in.)	Brick (ft.)	CI (ft.)	CSP (ft.)	VSP (ft.)	Total (ft.)
6		249.8	197.7		447.5
8			3851.0	8474.8	12325.8
10			2375.4	545.1	2920.5
12			1577.6	271.6	1849.2
15			366.4	147.8	514.2
16				1229.1	1229.1
24	437.6				437.6
30			488.4		488.4
38				247.6	247.6
48			982.4		982.4
54			829.2		829.2
60			3523.1		3523.1
72	1795.4				1795.4
Total	2233.0	249.8	14191.2	10916.0	27590.0

TABLE 24
Total Length of Sewer Pipelines in Tanner Drainage Basin within Poor Soil and MMI = XI Region under SES

Dia. (in.)	Brick (ft.)	CI (ft.)	CSP (ft.)	MONOCSP (ft.)	VSP (ft.)	Total (ft.)
6			496.1		1634.1	2130.2
8		228.1	13475.8		20685.2	34389.1
9					11299.6	11299.6
10			3839.0		15862.2	19701.2
12			6129.0		18097.0	24226.0
14					6336.5	6336.5
15			2914.1			2914.1
16					871.2	871.2
18			1539.9		1345.3	2885.2
20					192.3	192.3
21			3536.3			3536.3
24			1819.0	1307.9	1546.2	4673.1
27			265.0			265.0
30	719.6		1691.5	252.0		2663.1
36			3164.1	286.0		3450.1
38			3877.9			3877.9
48			504.4			504.4
72	4143.5			1542.5		5686.0
78				1660.8		1660.8
Total	4863.1	228.1	43252.1	5049.2	77869.6	131262.1

TABLE 25
Water Pipeline Replacement Estimates in Tanner Basin
within Good Soil and MMI = XI Region under SES

Dia. (in.)	**CI $**	**DI $**	**STL $**	**Total $**
2	2728.11	4119.61		6847.72
4	3565.98	3909.40		7475.38
6	44296.89	18553.92		62850.81
8	19577.80	110.44		19688.24
10	6024.15			6024.15
12	11047.74	7576.80	4198.26	22822.80
16		1896.60		1896.60
18				
20				
24				
30				
32				
36				
Total	$87,240.67	$36,166.77	$4,198.26	$127,605.70

TABLE 26
Water Pipeline Replacement Estimates in Tanner Basin
within Poor Soil and MMI = XI Region under SES

Dia. (in.)	CI $	DI $	STL $	Total $
2	6787.66	2511.41	2570.15	11869.22
4	19022.52	3180.54		22203.06
6	228980.73	11006.82		239987.55
8	248542.36	16103.12		264645.48
10	98613.35			98613.35
12	163586.28	9548.22	3006.30	176140.80
16	24198.18		6901.71	31099.89
18	3708.31			3708.31
20	113618.10			113618.10
24	30249.00	18420.00	33082.00	81751.00
30	154202.29			154202.29
32	33194.70			33194.70
36	98375.75			98375.75
Total	$1,223,079.23	$60,770.11	$45,560.16	$1,329,409.50

TABLE 27
Water Pipeline Replacement Estimates in Tanner Basin
within Poor & Good Soil and MMI = XI Region under SES

Dia. (in.)	CI $	DI $	STL $	Total $
2	9515.77	6631.02	2570.15	18716.94
4	22588.50	7089.94		29678.44
6	273277.62	29560.74		302838.36
8	268120.16	16213.56		284333.72
10	104637.50			104637.50
12	174634.02	17125.02	7204.56	198963.60
16	24198.18	1896.60	6901.71	32996.49
18	3708.31			3708.31
20	113618.10			113618.10
24	30249.00	18420.00	33082.00	81751.00
30	154202.29			154202.29
32	33194.70			33194.70
36	98375.75			98375.75
Total	$1,310,319.90	$96,936.88	$49,758.42	$1,457,015.20

TABLE 28
Sewer Pipeline Replacement Estimates in Tanner Basin
within Good Soil and MMI = XI Region under SES

Dia. (in.)	Brick $	CI $	CSP $	VSP $	Total $
6		1498.80	1186.20		2685.00
8			26957.00	59323.60	86280.60
9					
10			21378.60	4905.90	26284.50
12			15776.00	2716.00	18492.00
14					
15			4213.60	1699.70	5913.30
16				14134.65	14134.65
18					
20					
21					
24	12909.20				12909.20
27					
30			11233.20		11233.20
36					
38				7873.68	7873.68
48			42243.20		42243.20
54			41045.40		41045.40
60			197293.60		197293.60
72	149915.90				149915.90
78					
Total	$162,825.10	$1,498.80	$361,326.80	$90,653.53	$616,304.23

TABLE 29
Sewer Pipeline Replacement Estimates in Tanner Basin
within Poor Soil and MMI = XI Region under SES

Dia. (in.)	Brick $	CI $	CSP $	MONOCSP $	VSP $	Total $
6			2976.60		9804.60	12781.20
8		1596.70	94330.60		144796.40	240723.70
9					90396.80	90396.80
10			34551.00		142759.80	177310.80
12			61290.00		180970.00	242260.00
14					69701.50	69701.50
15			33512.15			33512.15
16					10018.80	10018.80
18			20018.70		17488.90	37507.60
20					2692.20	2692.20
21			51276.35			51276.35
24			29104.00	20926.40	24739.20	74769.60
27			5167.50			5167.50
30	26049.52		38904.50	5796.00		70750.02
36			93340.95	8437.00		101777.95
38			123317.22			123317.22
48			21689.20			21689.20
54						
60						
72	345982.20			107975.00		453957.25
78				127881.60		127881.60
Total	$372,031.72	$1,596.70	$609,478.77	$271,016.00	$693,368.20	$1,947,491.44

TABLE 30
Sewer Pipeline Replacement Estimates in Tanner Basin
within Good & Poor Soil Conditions, and MMI = XI Region under SES

Dia. (in.)	Brick $	CI $	CSP $	MONOCSP $	VSP $	Total $
6		1498.80	4162.80		9804.60	15466.20
8		1596.70	121287.60		204120.00	327004.30
9					90396.80	90396.80
10			55929.60		147665.70	203595.30
12			77066.00		183686.00	260752.00
14					69701.50	69701.50
15			37725.75		1699.70	39425.45
16					24153.45	24153.45
18			20018.70		17488.90	37507.60
20					2692.20	2692.20
21			51276.35			51276.35
24	12909.20		29104.00	20926.40	24739.20	87678.80
27			5167.50			5167.50
30	26049.52		50137.70	5796.00		81983.22
36			93340.95	8437.00		101777.95
38			123317.22		7873.68	131190.90
48			63932.40			63932.40
54			41045.40			41045.40
60			197293.60			197293.60
72	495898.10			107975.00		603873.15
78				127881.60		127881.60
Total	$534,856.82	$3,095.50	$970,805.57	$271,016.00	$784,021.73	$2,563,795.67

CONCLUSIONS

This paper has developed the loss estimation model for buried pipelines under various seismic environments and the GIS applications to Tanner and Fiske Drainage Basins of Portland, Oregon.

With the current GIS technology, the speedy data manipulations and retrieval capability, the potential loss of a water and sewer network (or replacement cost) can be estimated in a timely manner, under various earthquake intensities and soil liquefaction potentials. With the system being implemented on a PC based computer, it can be adopted to a small to moderate-sized city.

If a higher grade PC with a 386 or 486 instead of 286 machine is used and equipped with a fast drawing generation device such as Nth engine, sufficient RAM and disk space, the GIS applications and the loss estimation algorithm can be applied to large cities without difficulty.

In summary, the developed inventory and seismic loss estimation of water and sewer systems for Portland, Oregon would provide a tool for any city engineer, official and emergency response personnel to identify the critical areas for the pre-earthquake preparation and retrofitting the systems. The model can also help city decision makers to quickly set the priority for a post-earthquake damage survey, repair or restoration under the emergency situation.

No attempt has been made to be all inclusive in the facilities, replacement costs, and losses. The attempt has been made to demonstrate that these means and methods are workable and can be used by others to approach an analysis of their situation for expected earthquake losses.

Portland is now recognized by the scientific community as an area within an earthquake hazard region. The future actions of communities subjected to earthquake hazard will be played out in the coming years.

RECOMMENDATIONS

The results of this element of the study can be used for four specific activities:

1. To encourage the City of Portland water and sewage systems to expand the database scope to other basins.
2. As a guide and example to other cities to develop data bases, facility inventories, and replacement costs where earthquakes can be a concern.
3. As a tool for preparedness planning and training for emergency responses.
4. As a means of increasing the awareness of the hazard in a wider audience in the community of lifeline providers.

ACKNOWLEDGEMENTS

This project has been supported by the United States Geological Survey (USGS) under the National Earthquake Hazard Reduction Program (NEHRP) grant number 14-08-0001-G1694, in cooperation with the City of Portland which provided in-kind service for the data collection and the study of application to Federal Emergency Disaster Declaration. The program Director at USGS is Dr. Elaine Padovani.

This project has been benefitted by the GIS softwares education grants from Generation 5 Technology, Inc. in Denver, Colorado which provides Geo/SQL and Autodesk, Inc in Sausalito, California, which provides AutoCAD for the project. Their contributions of the softwares have expedited the completion of this project.

The authors wish to thank the reviewers, Dr. Ian P. Madin and Dr. Author C. Tarr for their excellent suggestions to improve the quality of the paper.

The participation of Mr. Donald B. Ballantyne, Project Engineer of Kennedy/Jenks/Chilton and Mr. William M. Elliott, Water Utility Engineer of the Portland Bureau of Water Works, as Co-Principals of the project, and Dr. Ian P. Madin, Hazard Geologist of the Oregon Department of Geology and Mineral

Industries, and Dr. Derok Cornforth of Cornforth Consultants, as the project consultants are also acknowledged.

In addition, Mr. Yu Wang, Visiting Scholar from the Municipal Engineering Research Institute of Beijing has participated in the inventory methodology development; Mr. Sunny Au, a high school intern has helped the data entry and Mrs. Mary G. Carmone has typed the manuscript of this paper.

REFERENCES

1. Ballantyne, D., 1980, "Earthquake Design Criteria for Water Supply and Waste Water Systems," Tech. Report, Environmental Quality Systems Inc..
2. Ballantyne, D., 1989, "Earthquake Loss Estimation Modeling of the Seattle Water System," NEHRP summaries of the Technical Reports, XXVVIII, USGS, Open File Report 89-453, July, pp. 521-522.
3. Cornforth, D., 1986, "Mt. Tabor-Reservoir No. 6 Foundation Liquefaction Study," Tech. Report, Cornforth Consultants, Inc., January.
4. Couch, R.L. and R.E. Peterson, 1971, "Geological and Geophysical Factor Related to Portland International Airport Expansion," Tech. Report, Department of Geophysical Oceanography, Oregon State University.
5. EERI Investigation Team, 1989, "Loma Prieta Earthquake, October 17, 1989," Preliminary Reconnaissance Report, Earthquake Engineering Research Institute, November.
6. Eguchi, R.T., 1983, "Seismic Vulnerability Models for Underground Pipes," *Proc. of International Symposium on Lifeline Earthquake Engineering*, ASME, Portland, Oregon, June.
7. Eguchi, R.T., T. Philipson, and J. Wiggins, 1982, "An Approach for Evaluating the Earthquake Performance of Water Supply Systems," *Proc. of the Third International Earthquake Microzonation Conference*, Seattle, Washington, Vol. 3, pp. 1629-1640.
8. Facility Mapping System Inc., 1989, "Facility Mapping System for AutoCAD (FMS/AC)," Mill Valley, California.
9. General 5 Technology, Inc., 1989, "Geo/SQL," Denver, Colorado.
10. Katayama, T., K. Kubo, and M. Sato, 1975, "Earthquake Damage to Water and Gas Distribution Systems," *Proc. of U.S. National Conference on Earthquake Engineering*, June, pp. 396-405.
11. Kubo, K. and R. Isoyama, 1980, "Damage to Buried Utility Pipes in the 1987 Miyagi-Ken-Oki Earthquake," *Proc. of the 7th WCEE*, Istanbul, Vol. 8, Sept., pp. 225-232.
12. Madin, I.P., 1989, "Evaluating Earthquake Hazards in Portland, Oregon metropolitan Area: Mapping Potentially Hazardous Soils," Oregon Geology, Vol. 51, No. 5, September, pp. 106-110.
13. Okamoto, S., 1984, Introduction to Earthquake Engineering, 2nd Ed. University of Tokyo Press, Tokyo, Japan.
14. Rojahn, C. and R. Sharpe, 1985, "Earthquake Damage Evaluation Data for California," ATC-13, Applied Technology Council.
15. Seed, H.B. and I.M. Idriss, 1982, Ground Motions and Soil Liquefaction During Earthquakes, Earthquake Engineering Research Institute Monograph, EERI.
16. Taylor, C.E., 1986, "Earthquake Vulnerability of Water Supply and Natural Gas Systems," Tech. Report, NTS Engineering, May.
17. Taylor, C.E., 1988, "Continuing Investigations of Earthquake Risk to Utah Water and Gas Systems," NTS Engineering Report, March.
18. TCLEE, 1983, "Advisory Notes on Lifeline Earthquake Engineering," ASCE Report.
19. Wang, L.R.L., 1988, "Seismic Counter Measurers for Buried Pipelines," presented at the *ASCE Pipeline Div. Specialty Conference*, Boston, MA, June 6-7.
20. Wang, L.R.L., M. O'Rourke, and R. Pikul, 1979, "Seismic Vulnerability, Behavior, and Design of Buried Pipelines," Tech. Report, Civil Engineering Department, Rensselaer Polytechnic Institute.

21. Wang, L.R.L., S.P. Sun, and S. Shen, 1985, "Seismic Damage Behavior of Buried Lifeline Systems During Recent Severe Earthquakes in U.S., China and Other Countries," Tech. Report, ODU LEE-02, Old Dominion University, December.
22. Wiggins, J. H. and C. Taylor, 1986, "Damageability of Low-Rise Construction: Data Bases; Categorization Techniques; Rating Procedures; Proposed Survey Procedures", Report 1442, Vol. II. NTS Engineering, December.
23. Youd, T.L. and D.M. Perkins, 1978, "Mapping Liquefaction-Induced Ground Failure Potential," *Journal of The Geotechnical Engineering Division*, ASCE, Vol. 104, No. G74, April, pp.

FIGURE CAPTIONS

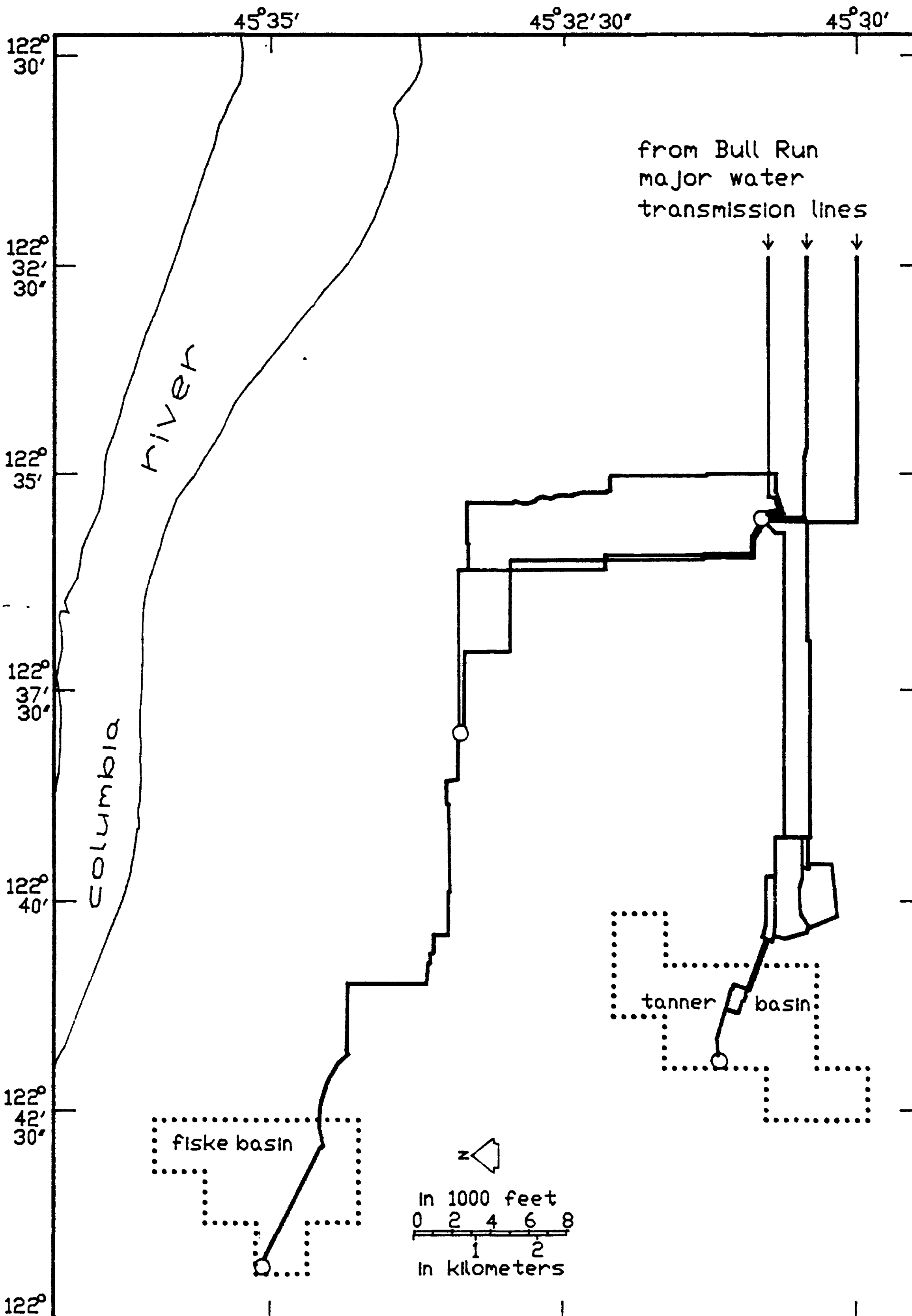

Figure 1. -- Portland Water Supply Systems

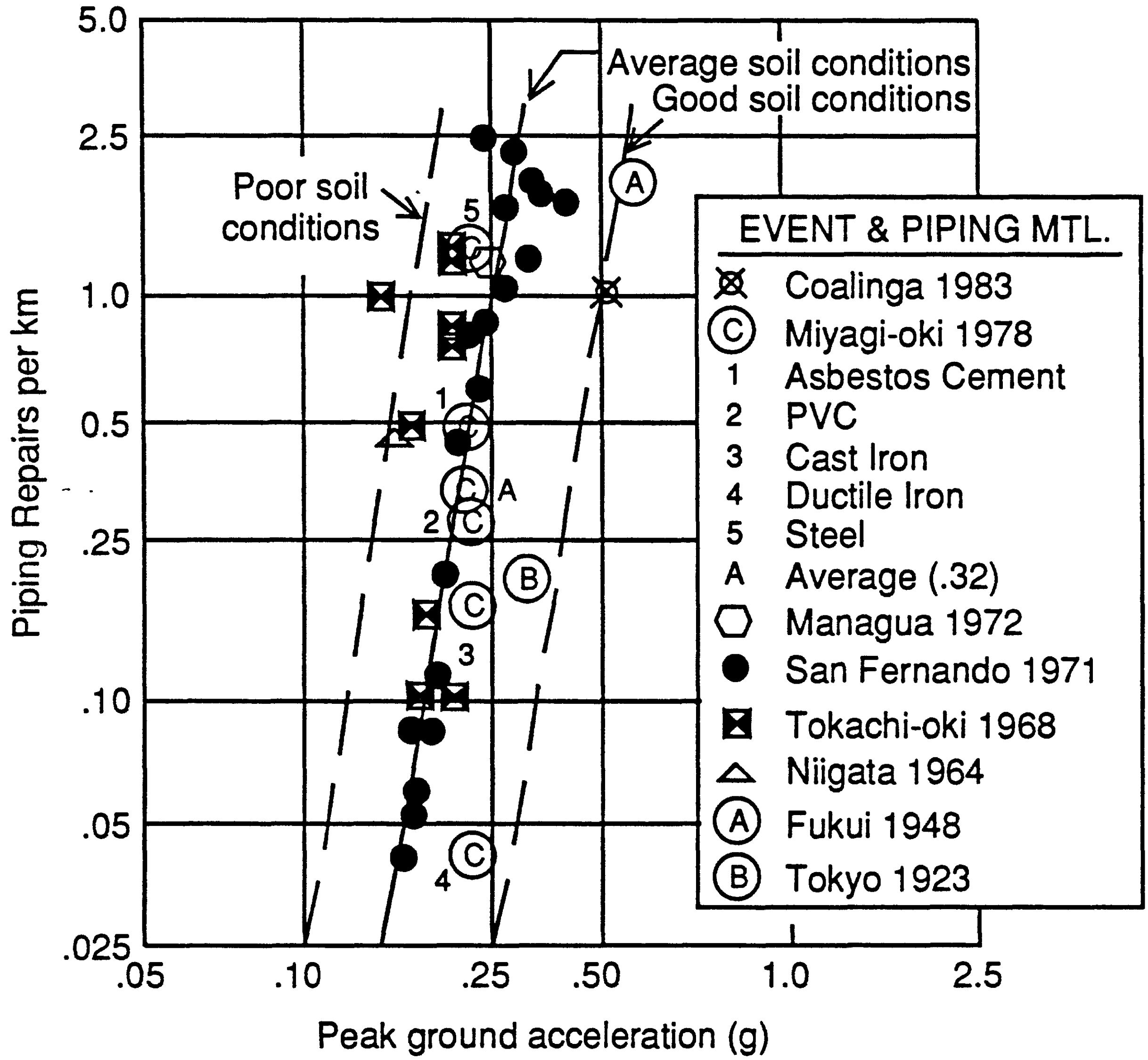

Figure 2. -- Repairs to Water Pipelines due to Wave Propagation Effects from Past Earthquakes

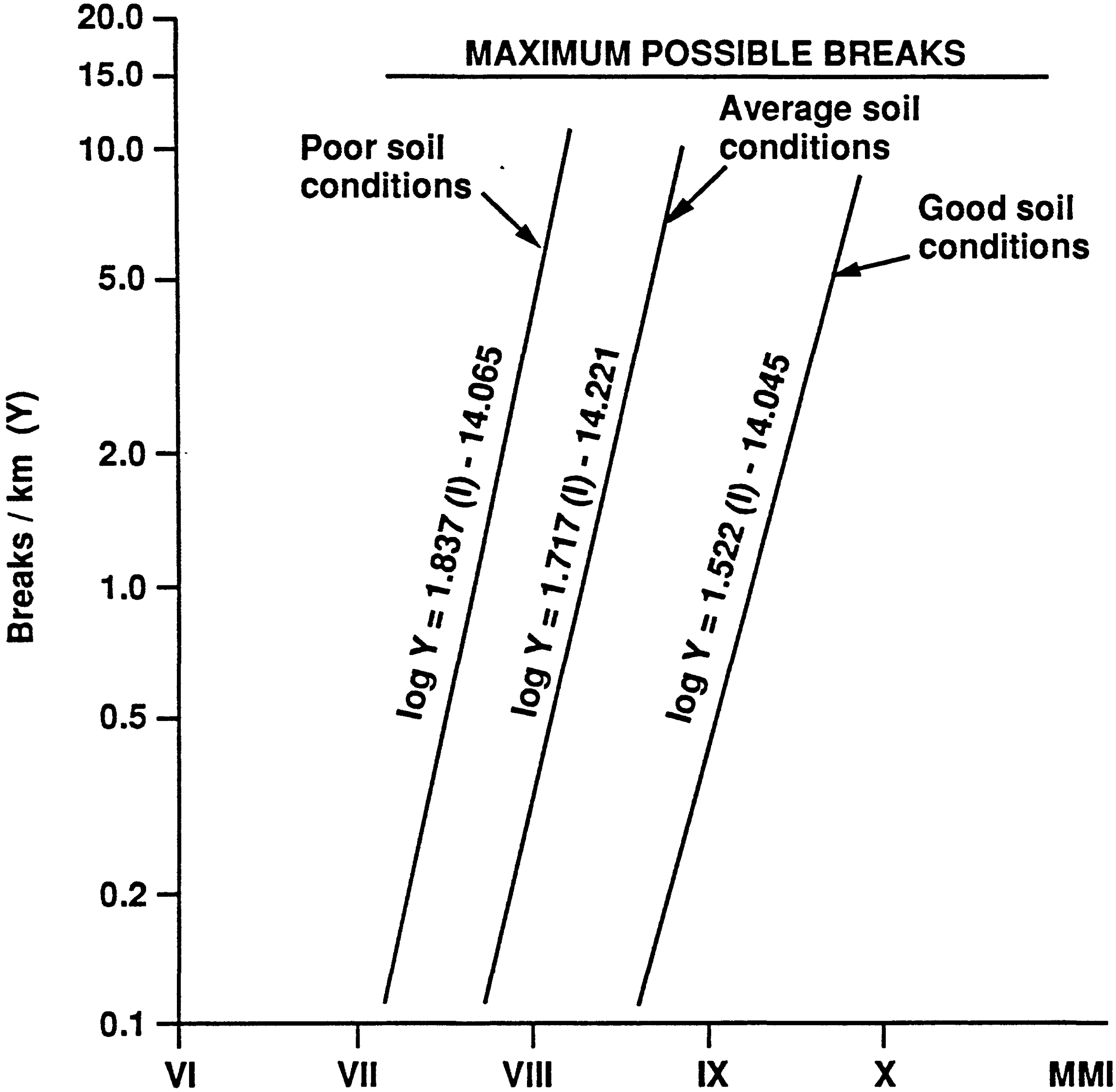

Figure 3. -- Pipeline Damage (breaks/km) Versus Intensity (MMI)

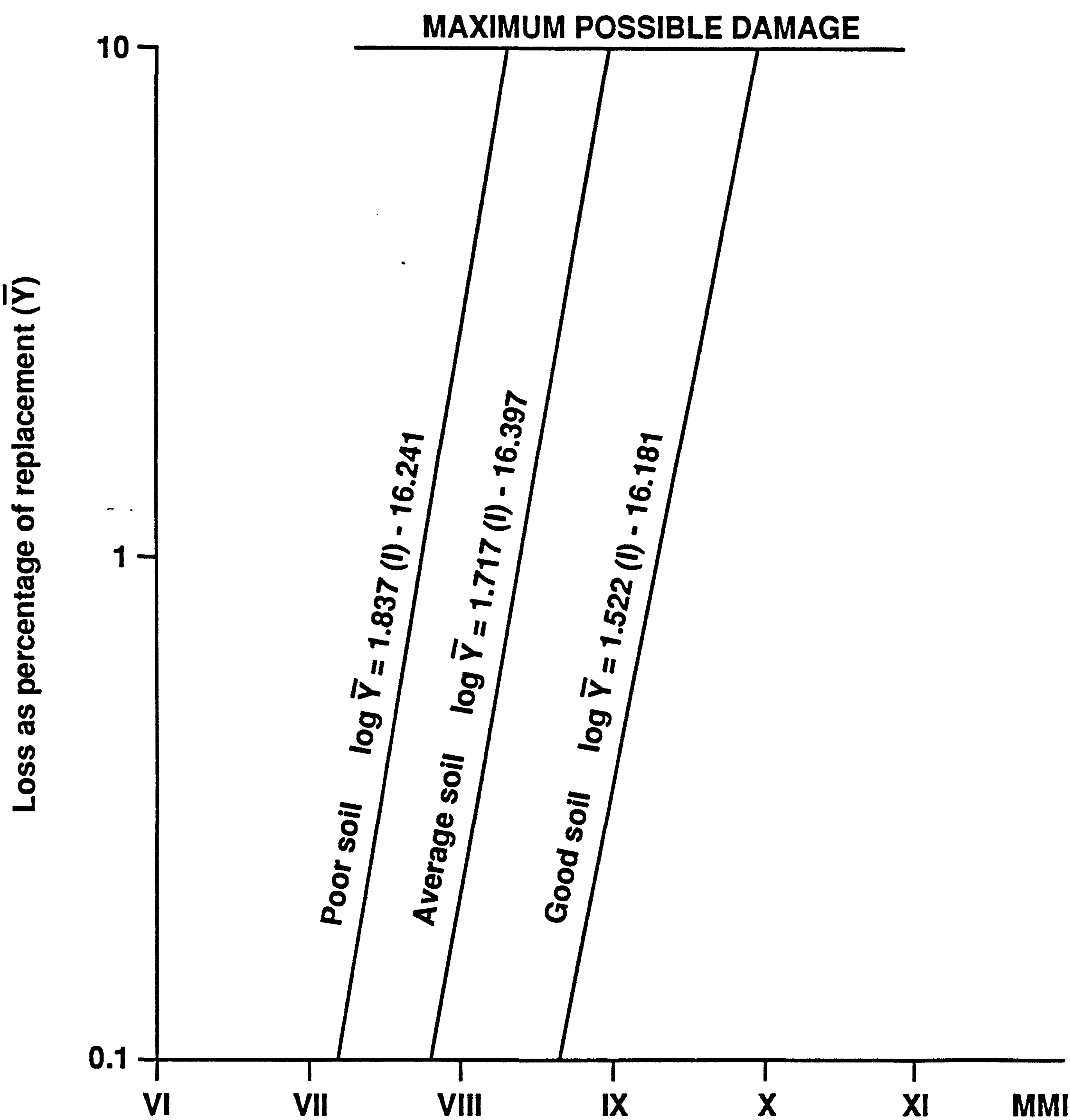

Figure 4. -- Pipeline Damage (percent loss) Versus Intensity (MMI)

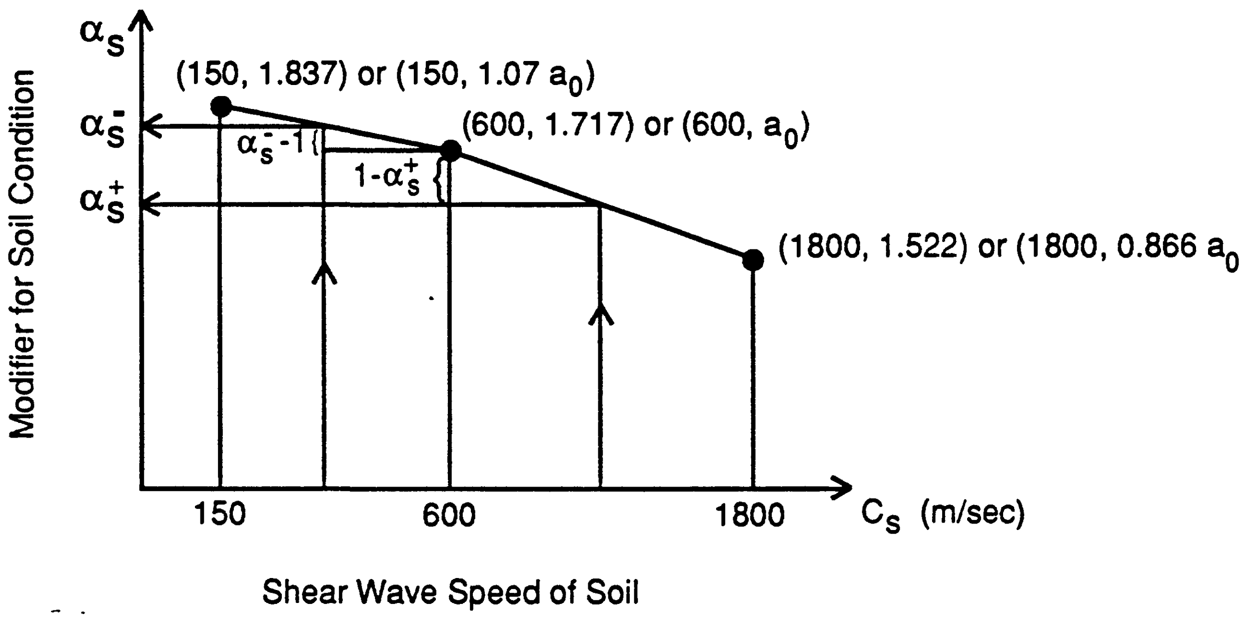

$$a_0 = 1.717$$

$$\frac{(\alpha_s^- - 1)\, a_0}{600 - C_s} = \frac{(1.07-1)\, a_0}{600-150} = 1.556 \times 10^{-4}\ a_0$$

$$\alpha_s^- = 1.093 - 1.556 \times 10^{-4}\, C_s$$

$$\frac{(1 - \alpha_s^+)\, a_0}{C_s - 600} = \frac{(1-0.886)\, a_0}{1800-600} = 9.5 \times 10^{-5}\ a_0$$

$$\alpha_s^+ = 1.057 - 9.5 \times 10^{-5}\, C_s$$

Figure 5. -- Slope Modification in Loss Algorithm for Soil Condition

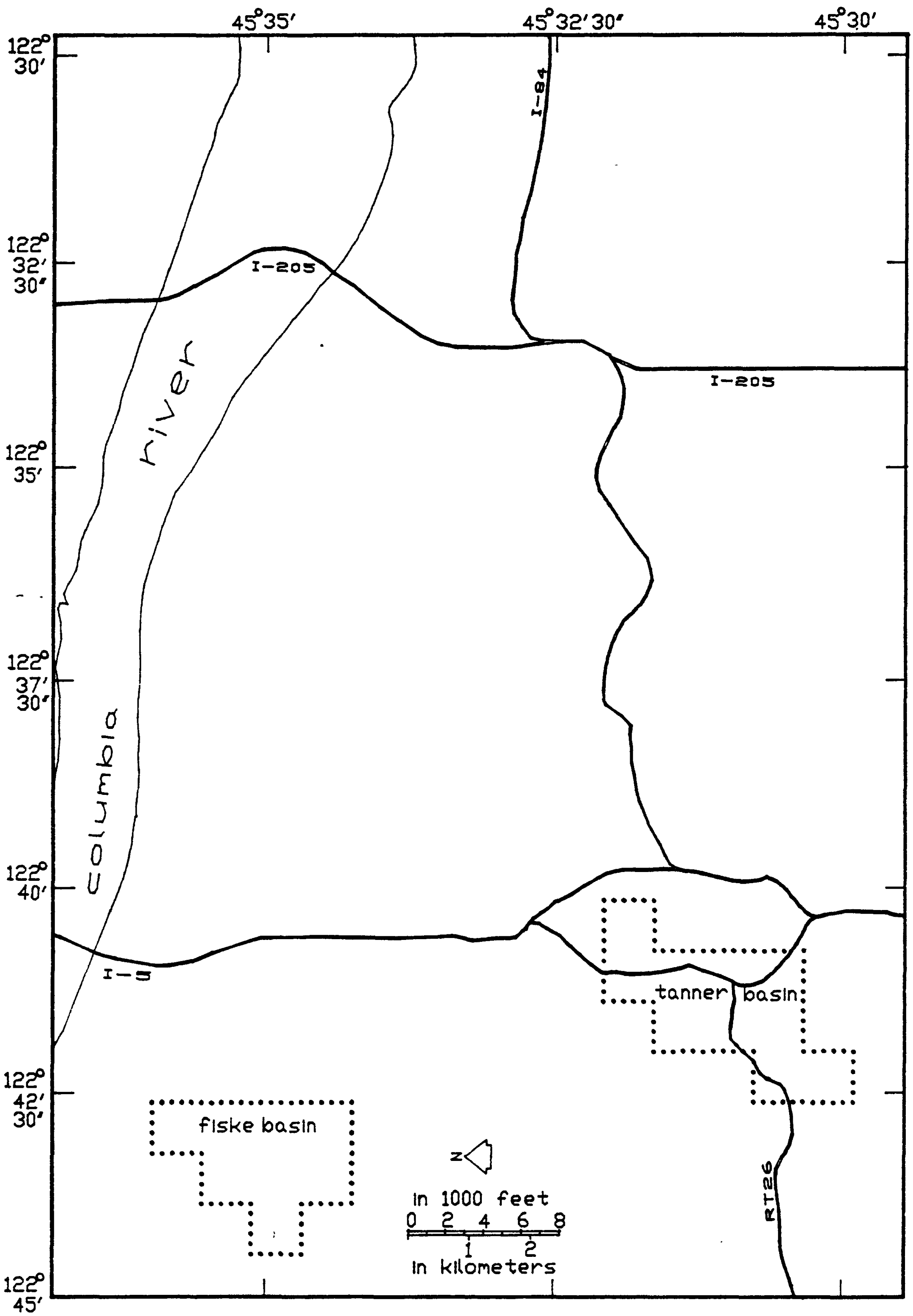

Figure 6. -- Study Scope and Common Factors Map

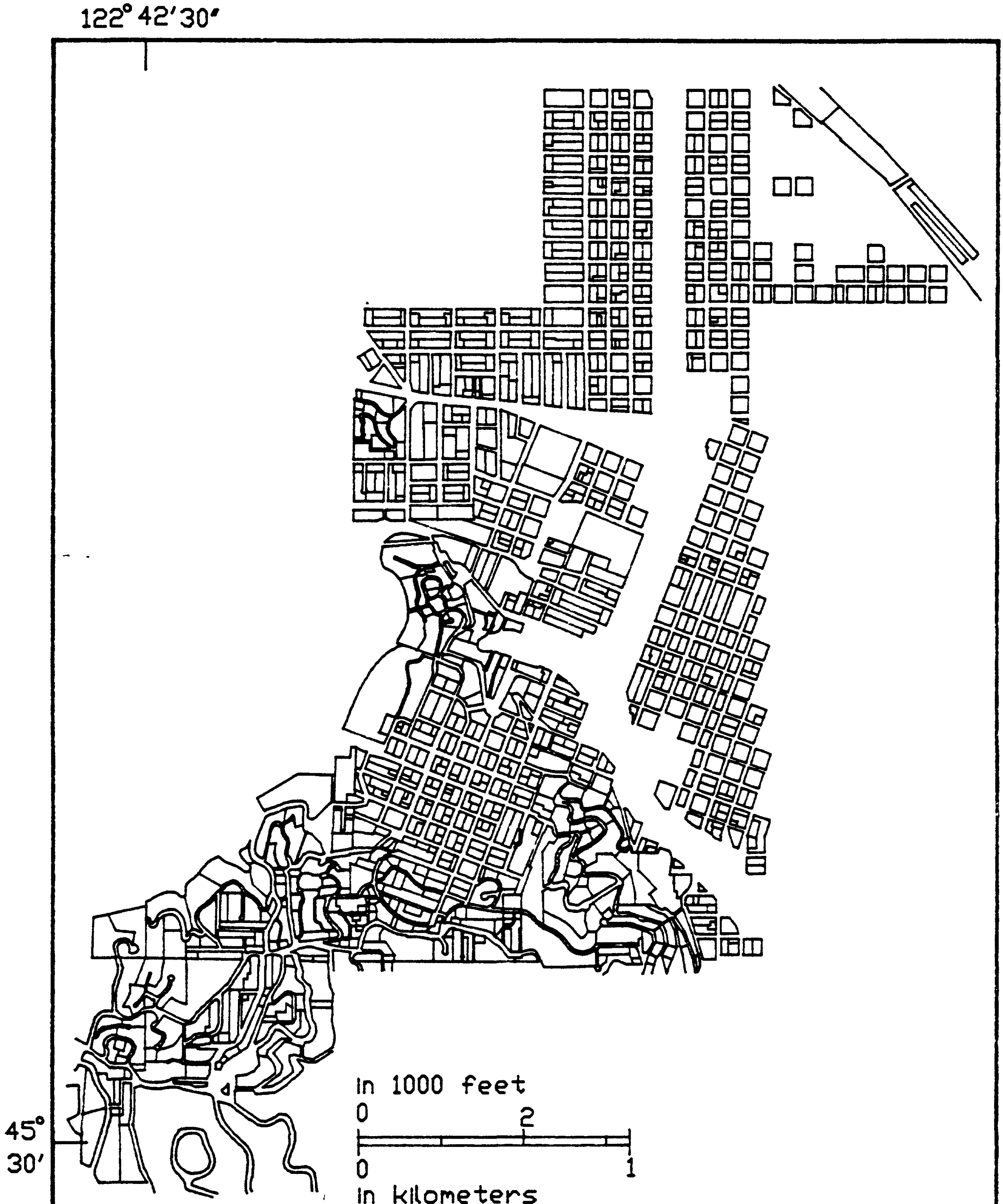

Figure 7. – Tanner Drainage Basin Parcel Database

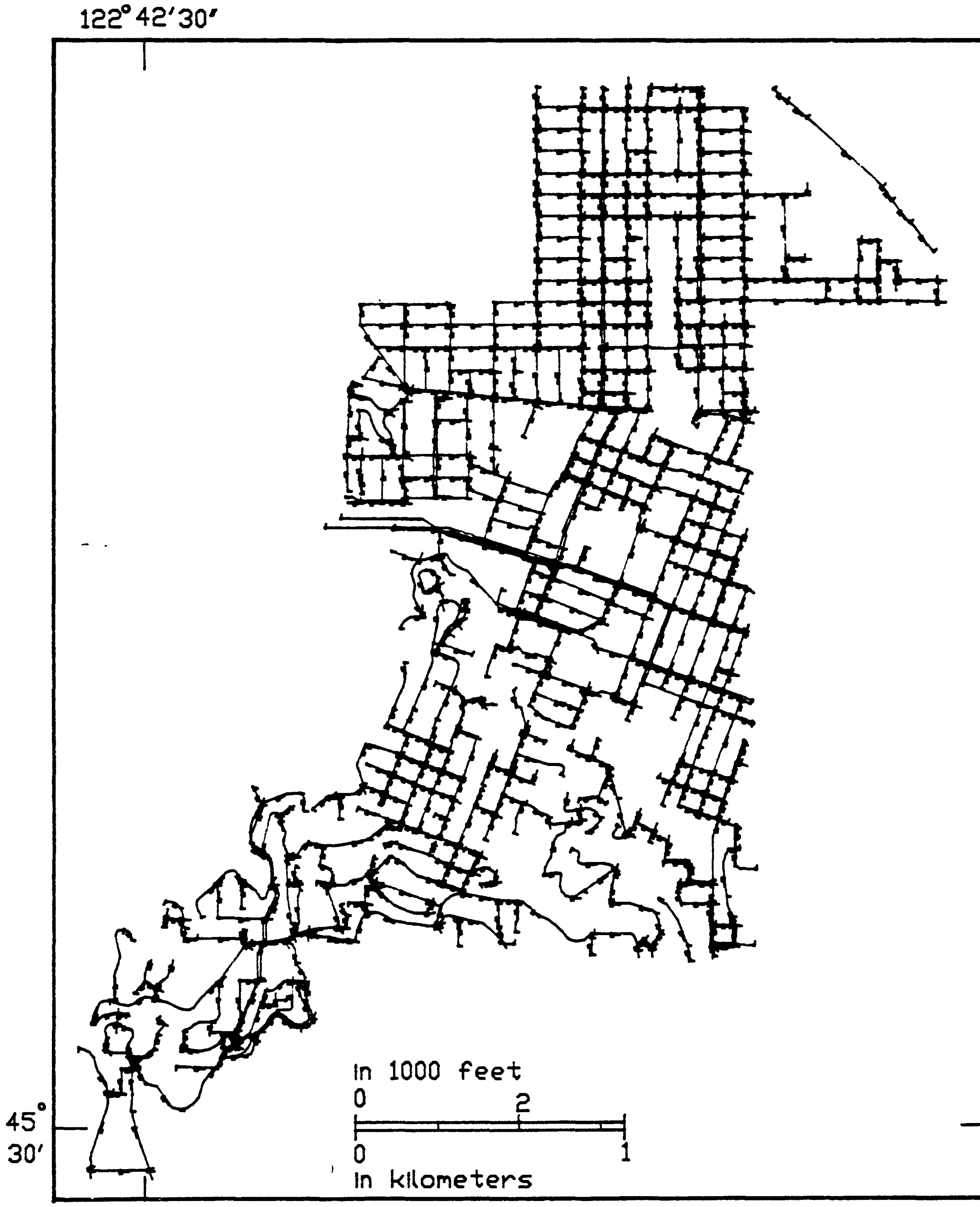

Figure 8. -- Tanner Drainage Basin Water Network Database

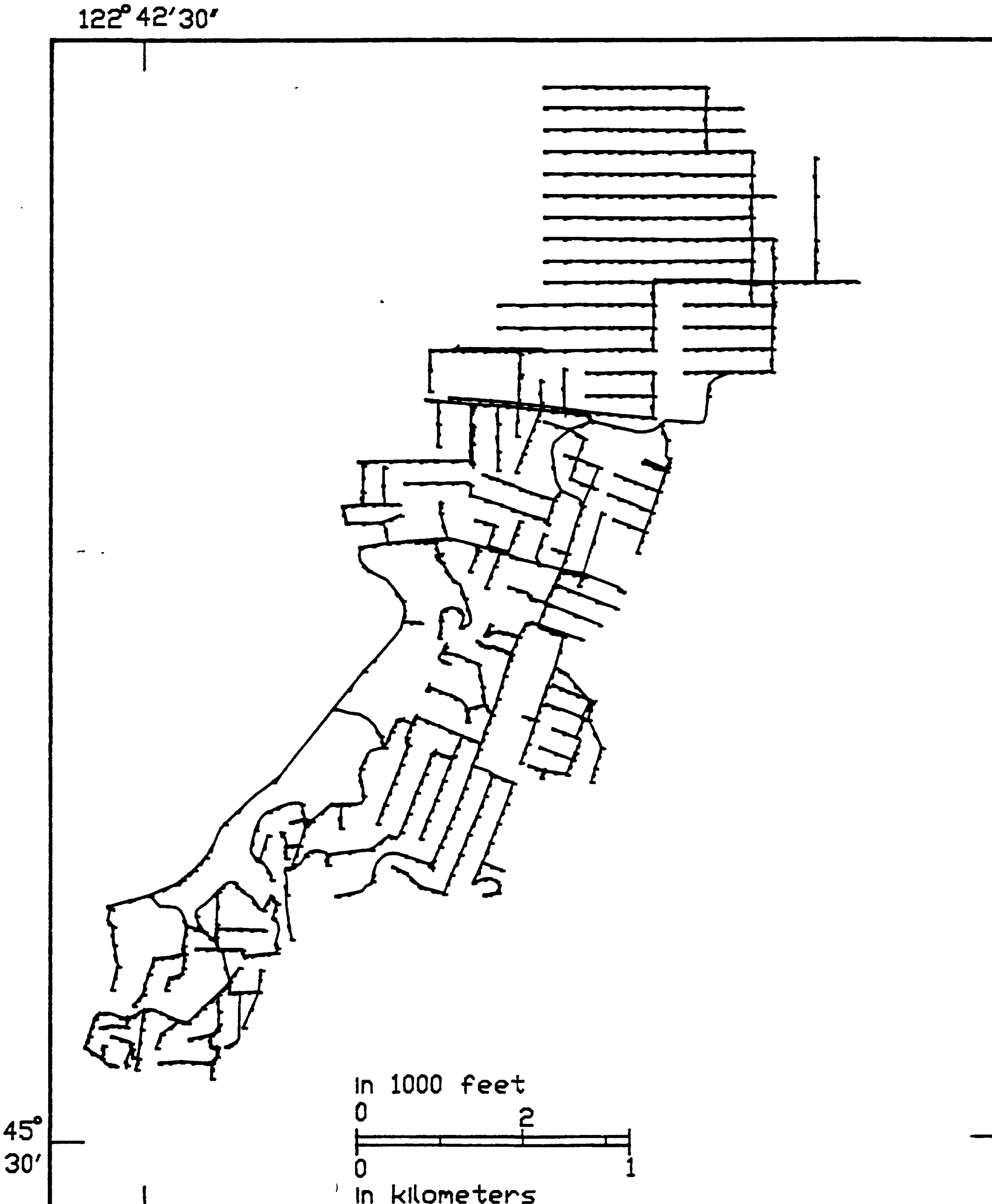

Figure 9. -- Tanner Drainage Basin Sewer Network Database

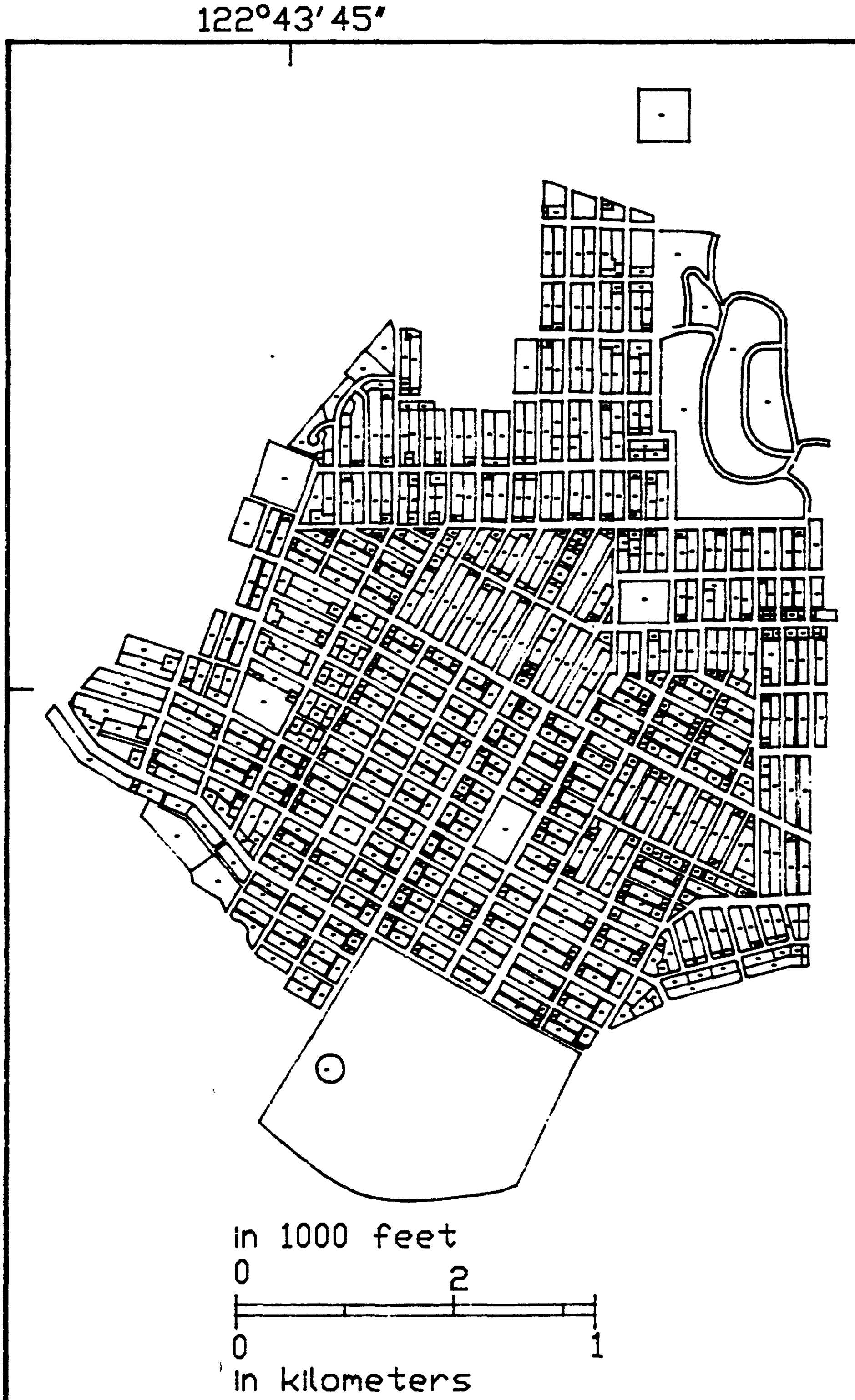

Figure 10. -- Fiske Drainage Basin Parcel Database

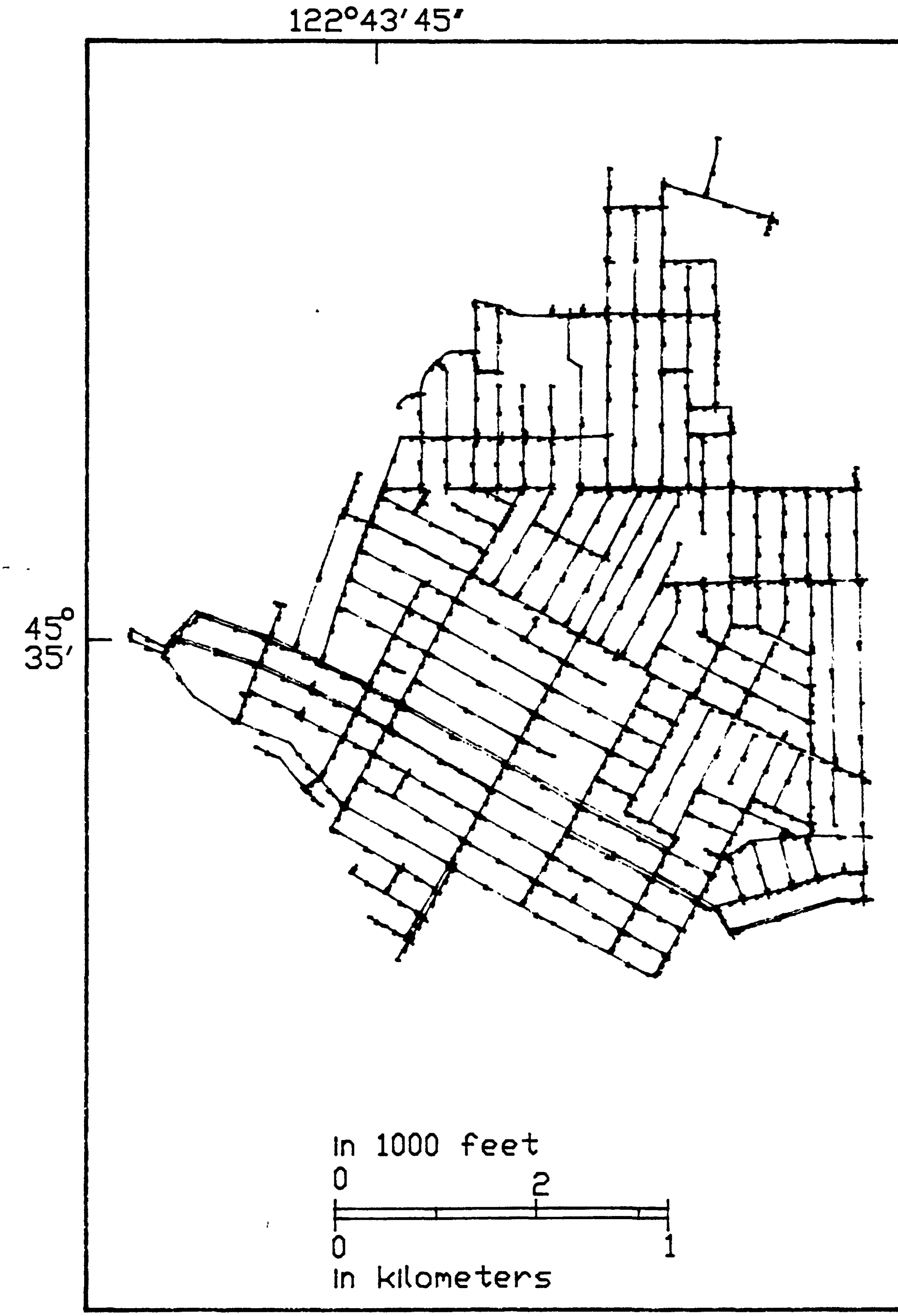

Figure 11. -- Fiske Drainage Basin Water Network Database

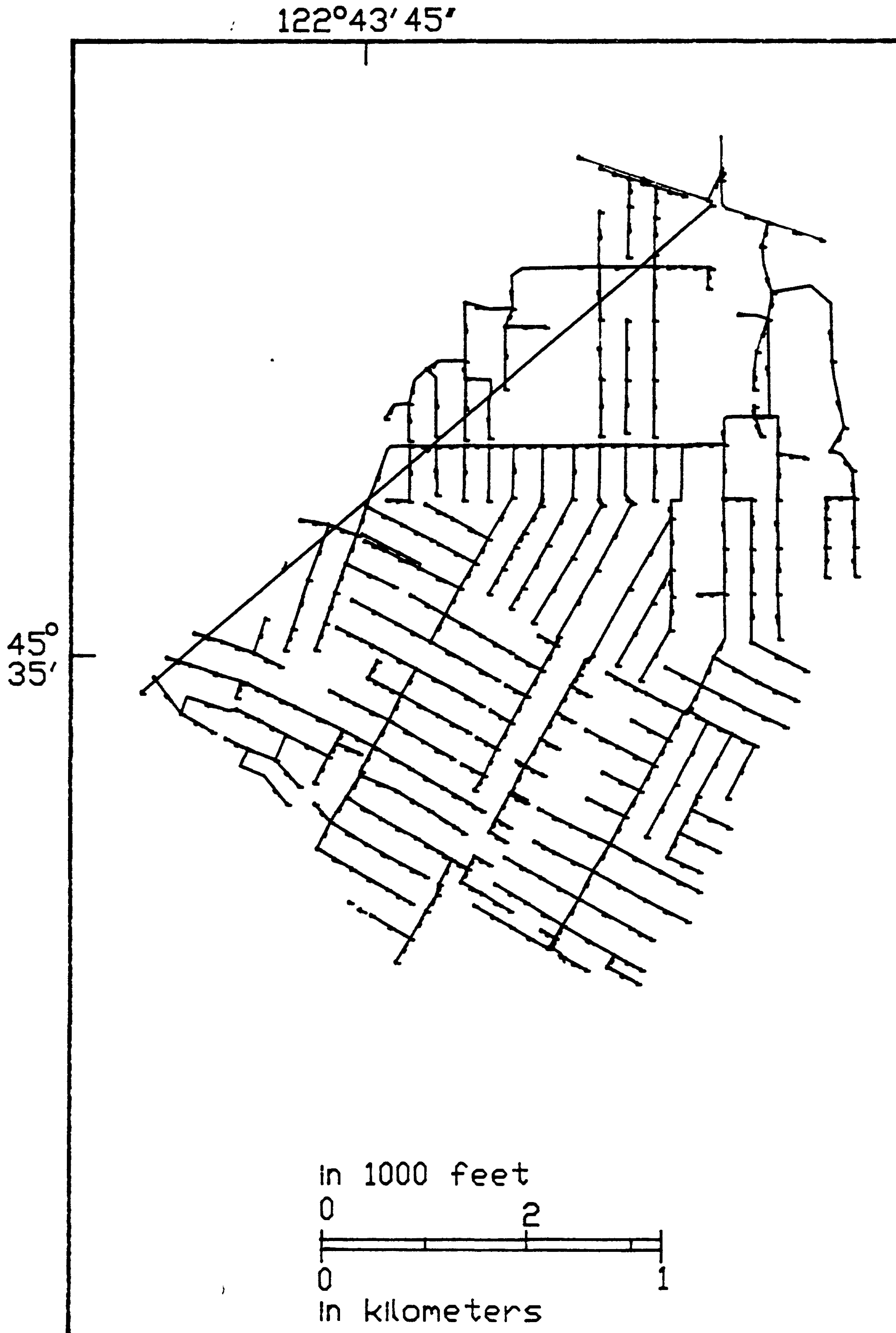

Figure 12. -- Fiske Drainage Basin Sewer Network Database

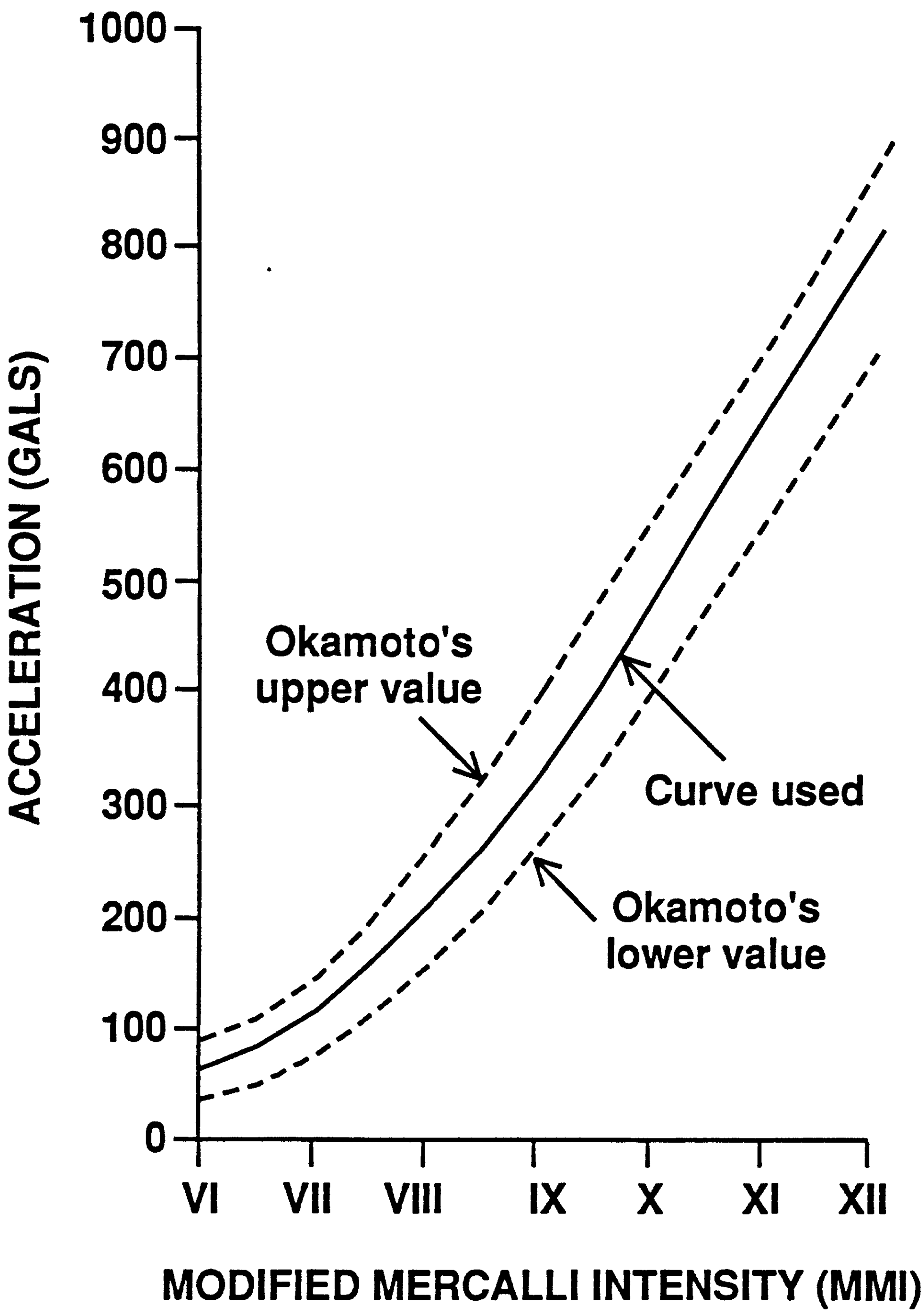

Figure 13. -- Okamoto's Peak Ground Acceleration and Earthquake Intensity (MMI) Relationship (1984)

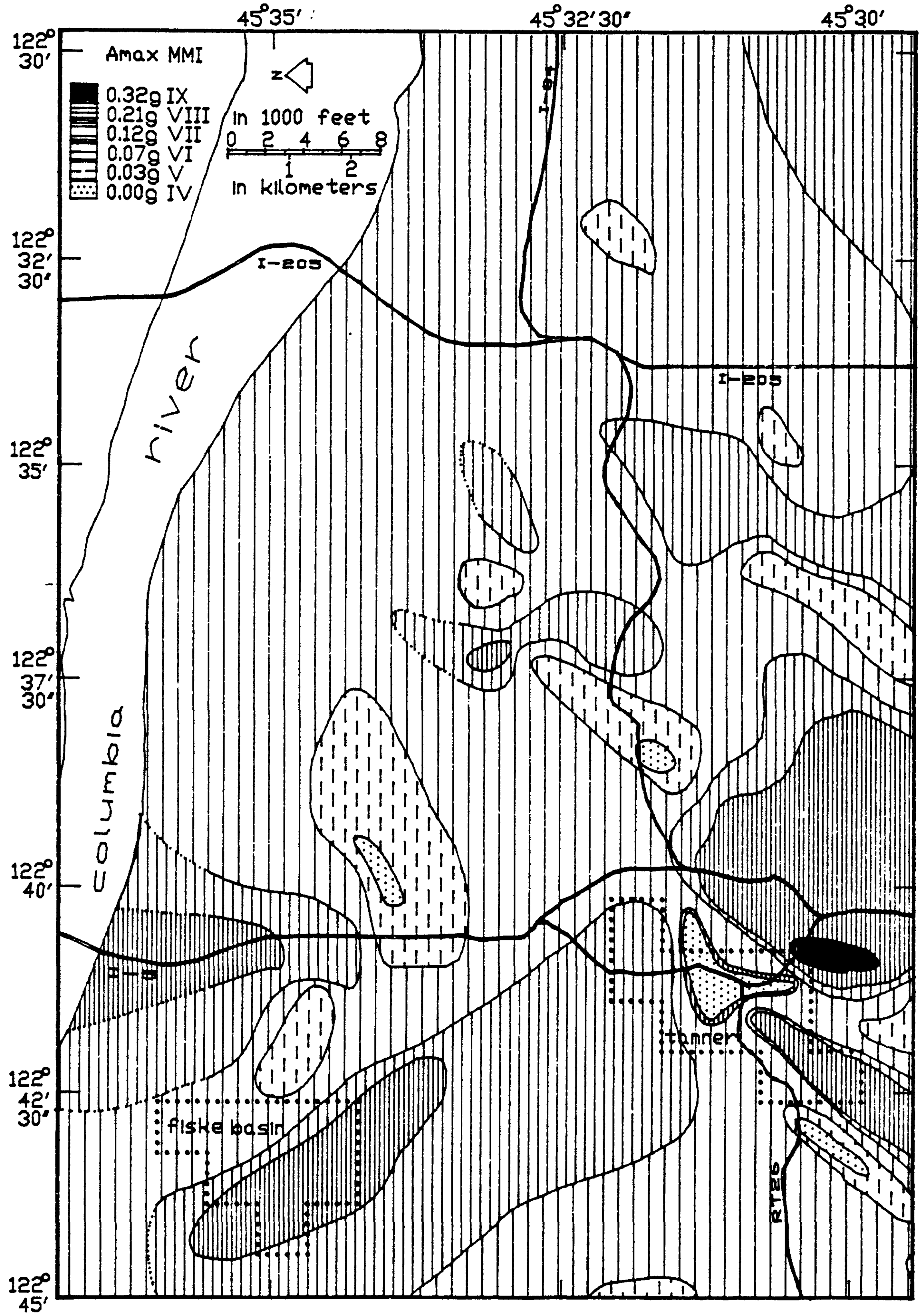

Figure 14. -- Seismic Intensity under Portland Local Earthquake Scenario

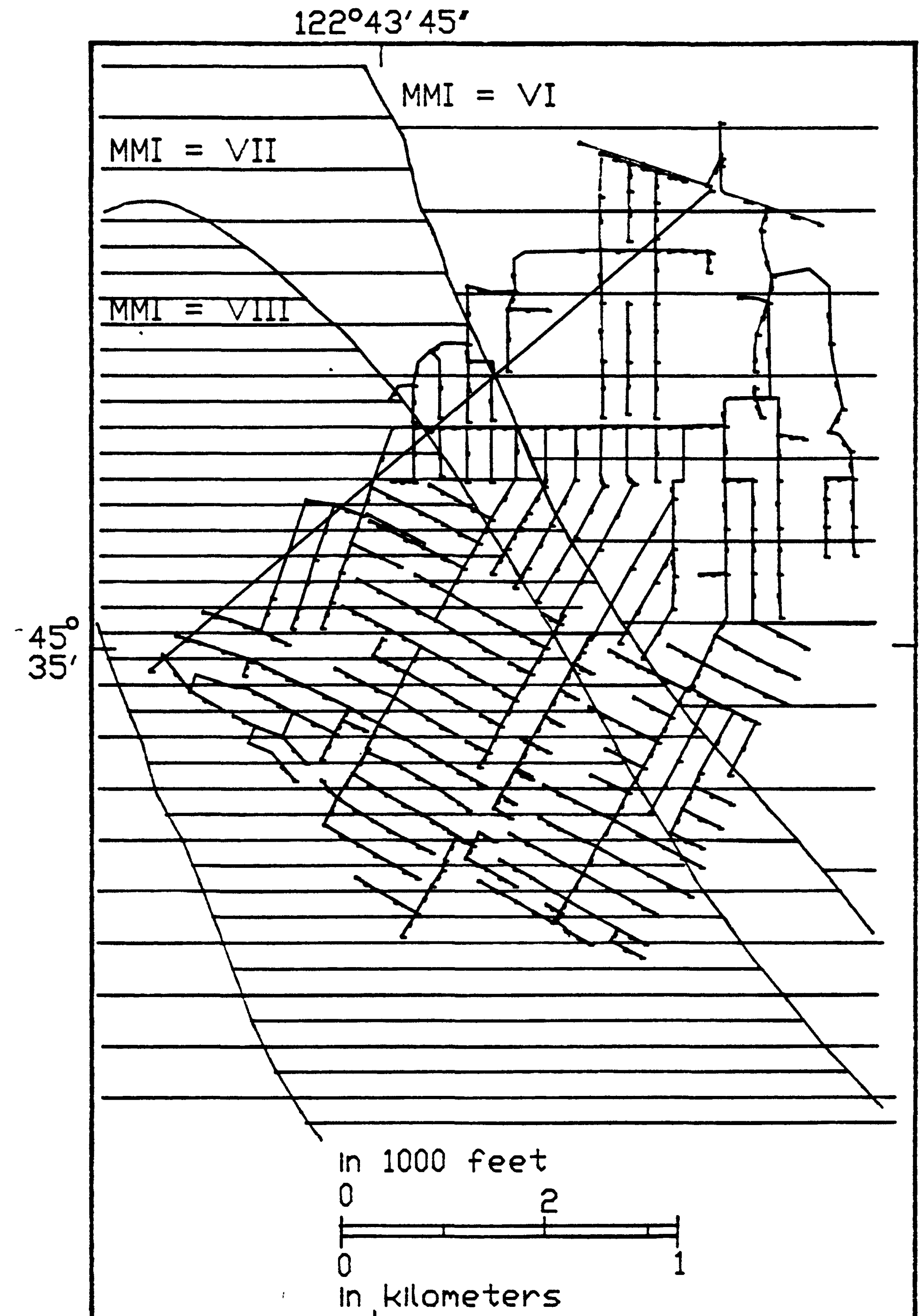

Figure 15. -- Fiske Drainage Basin Sewer Network versus MMI under Local Earthquake Scenario

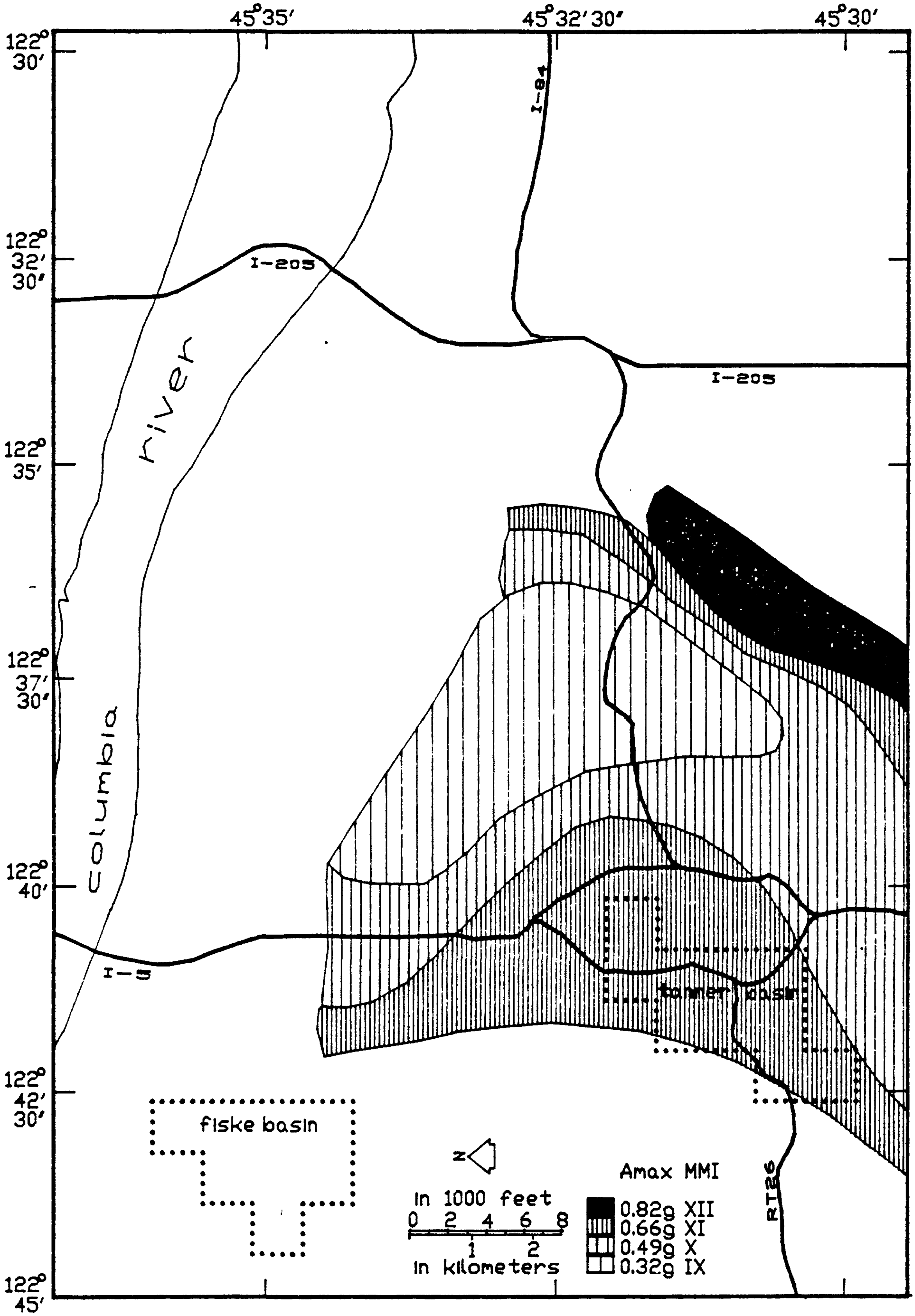

Figure 16. -- Seismic Intensity for Tanner Drainage Basin under Portland Subduction Earthquake Scenario

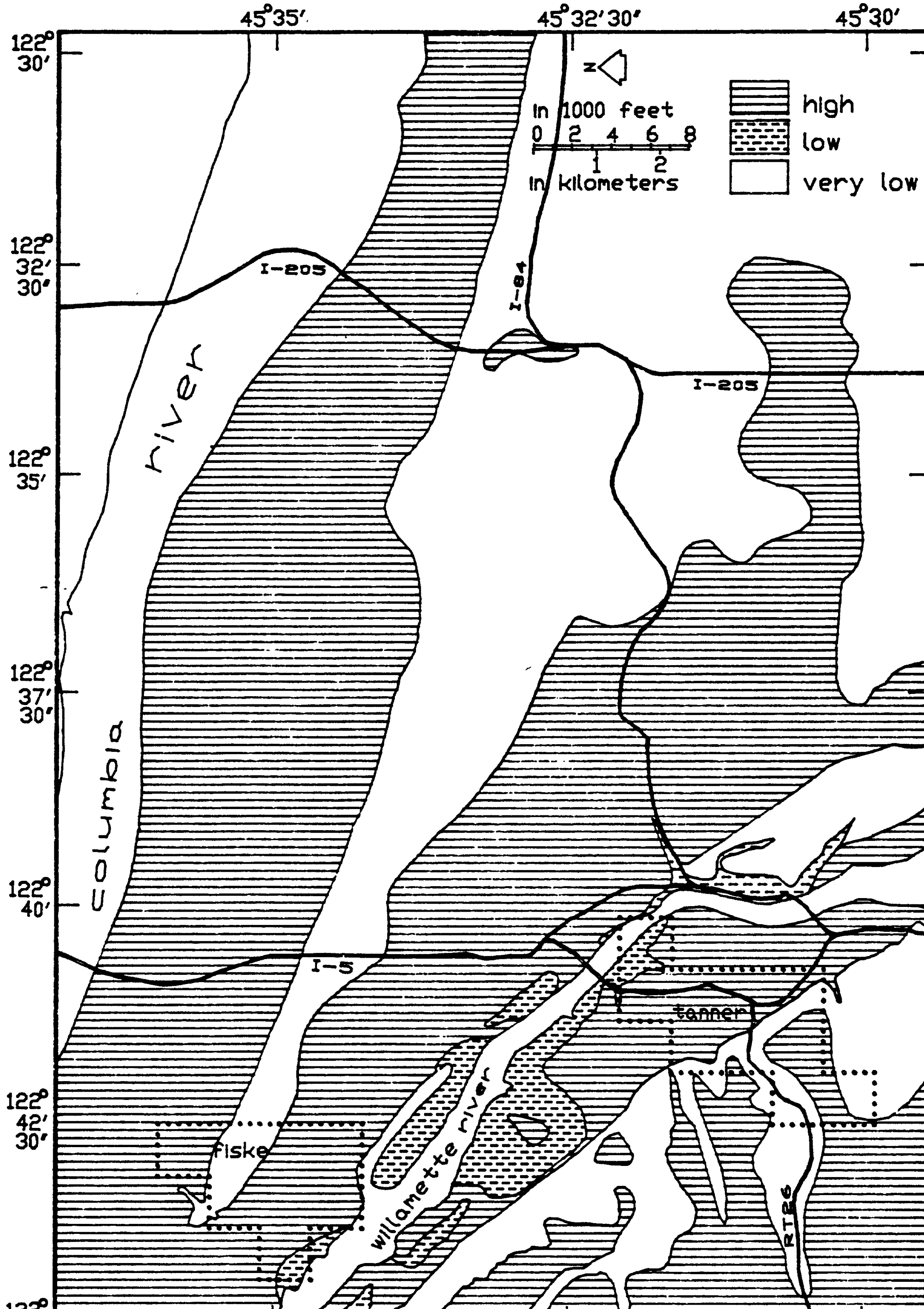

Figure 17. -- Surficial Soil Liquefaction Susceptibility

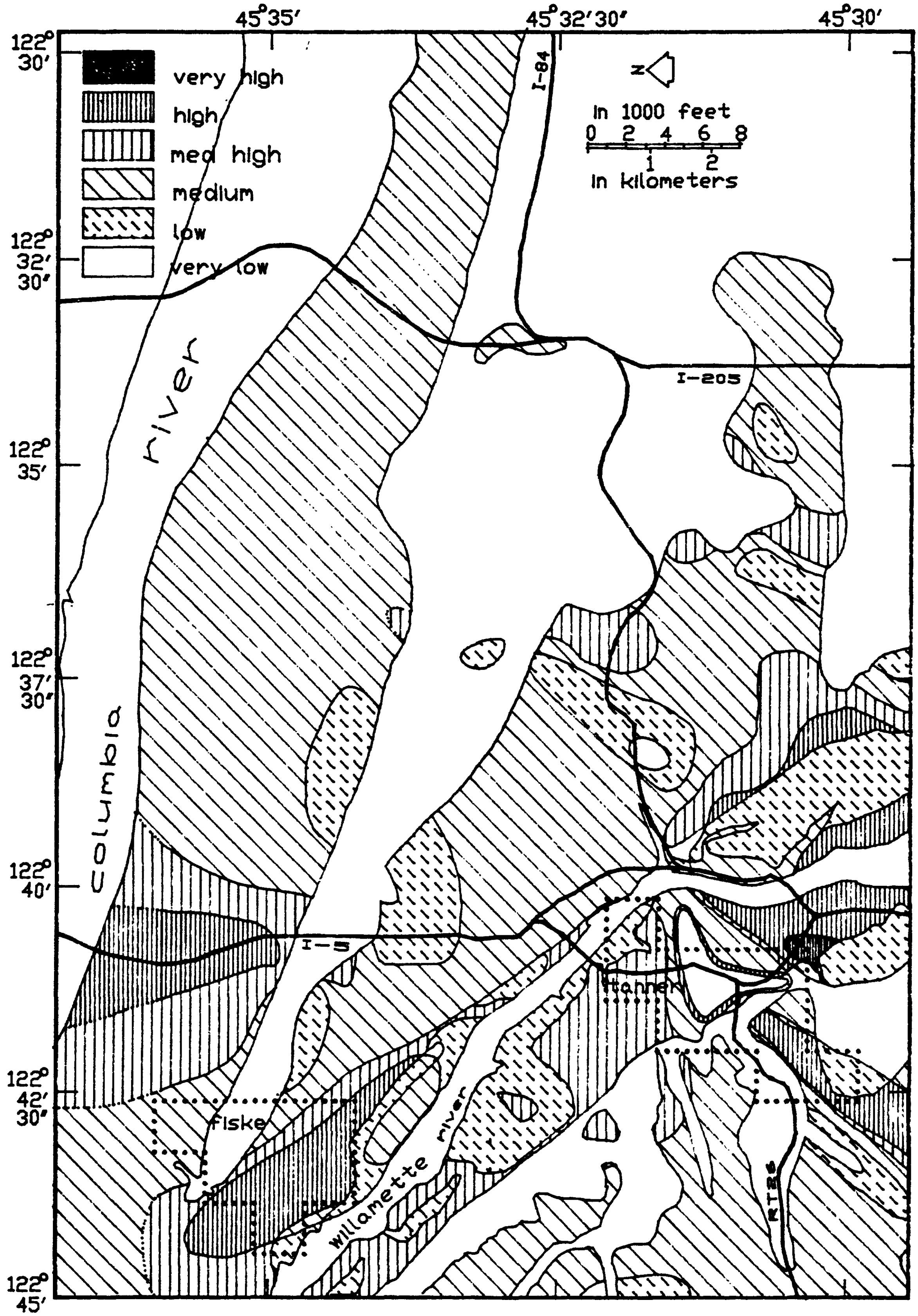

Figure 18. -- Liquefaction Potential Map for Portland under Local Earthquake Scenario

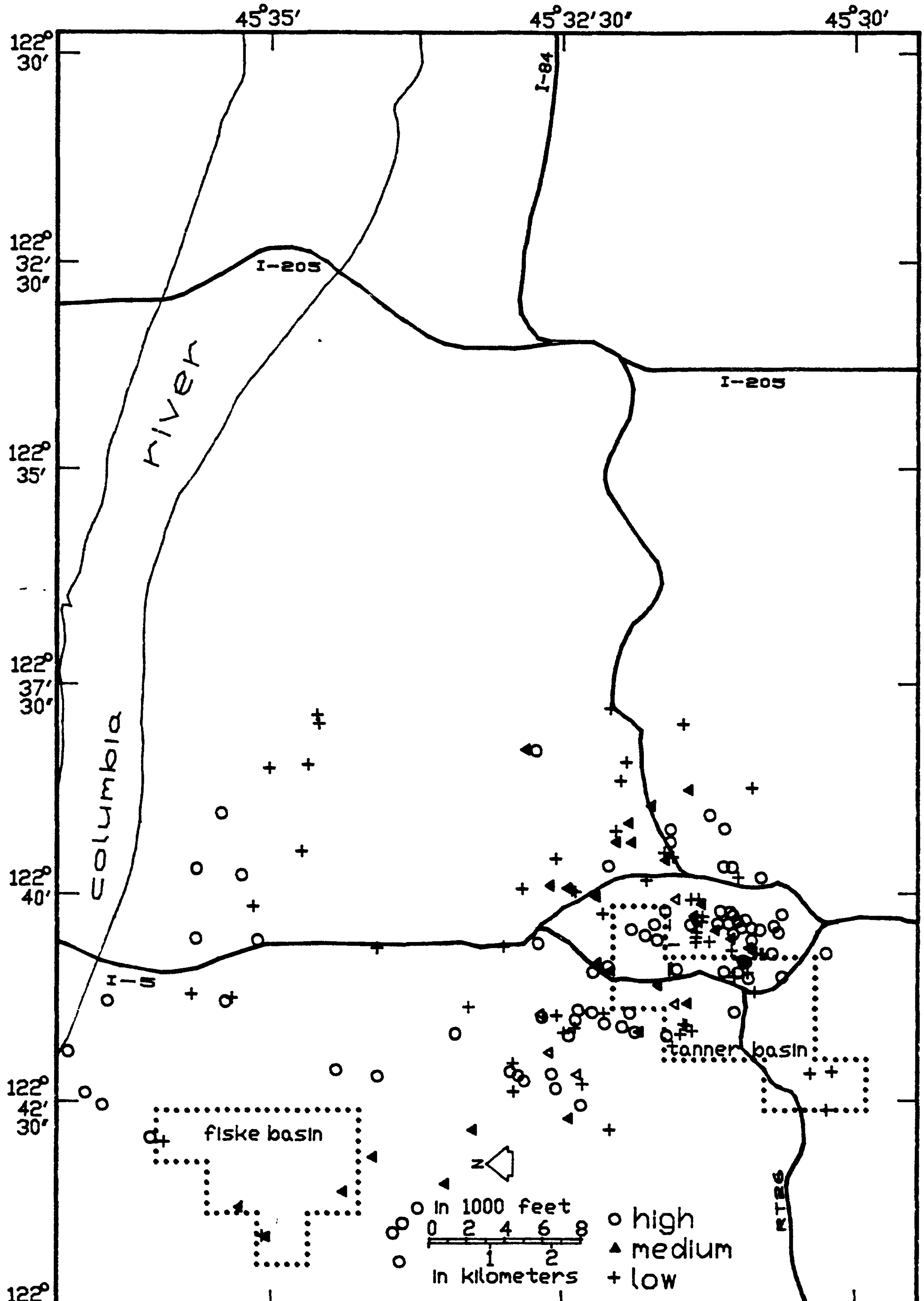

Figure 19. -- Detailed Liquefaction Potential Analysis on Boring Logs under Local Earthquake Scenario

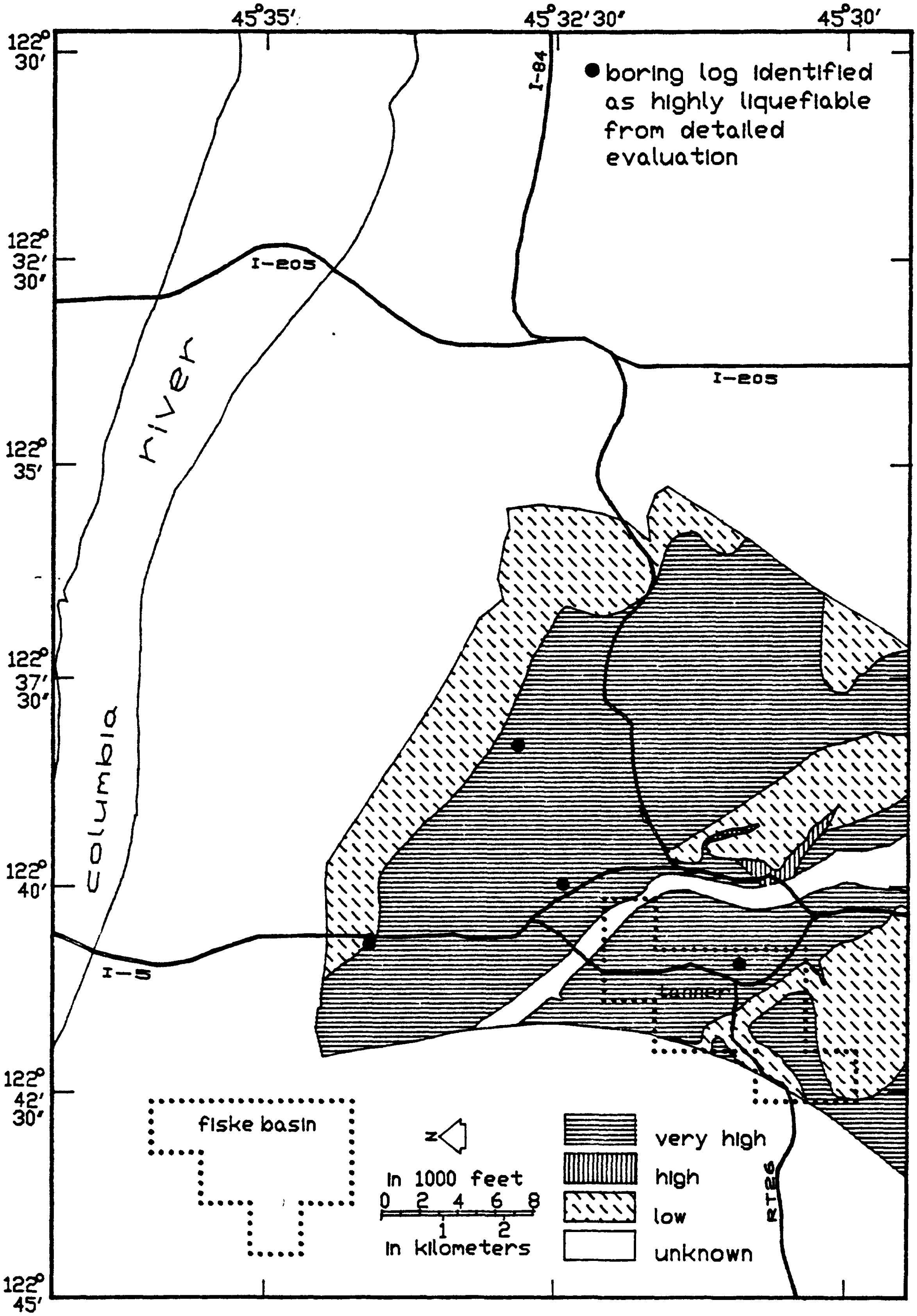

Figure 20. -- Liquefaction Potential Map for Portland under Subduction Earthquake Scenario

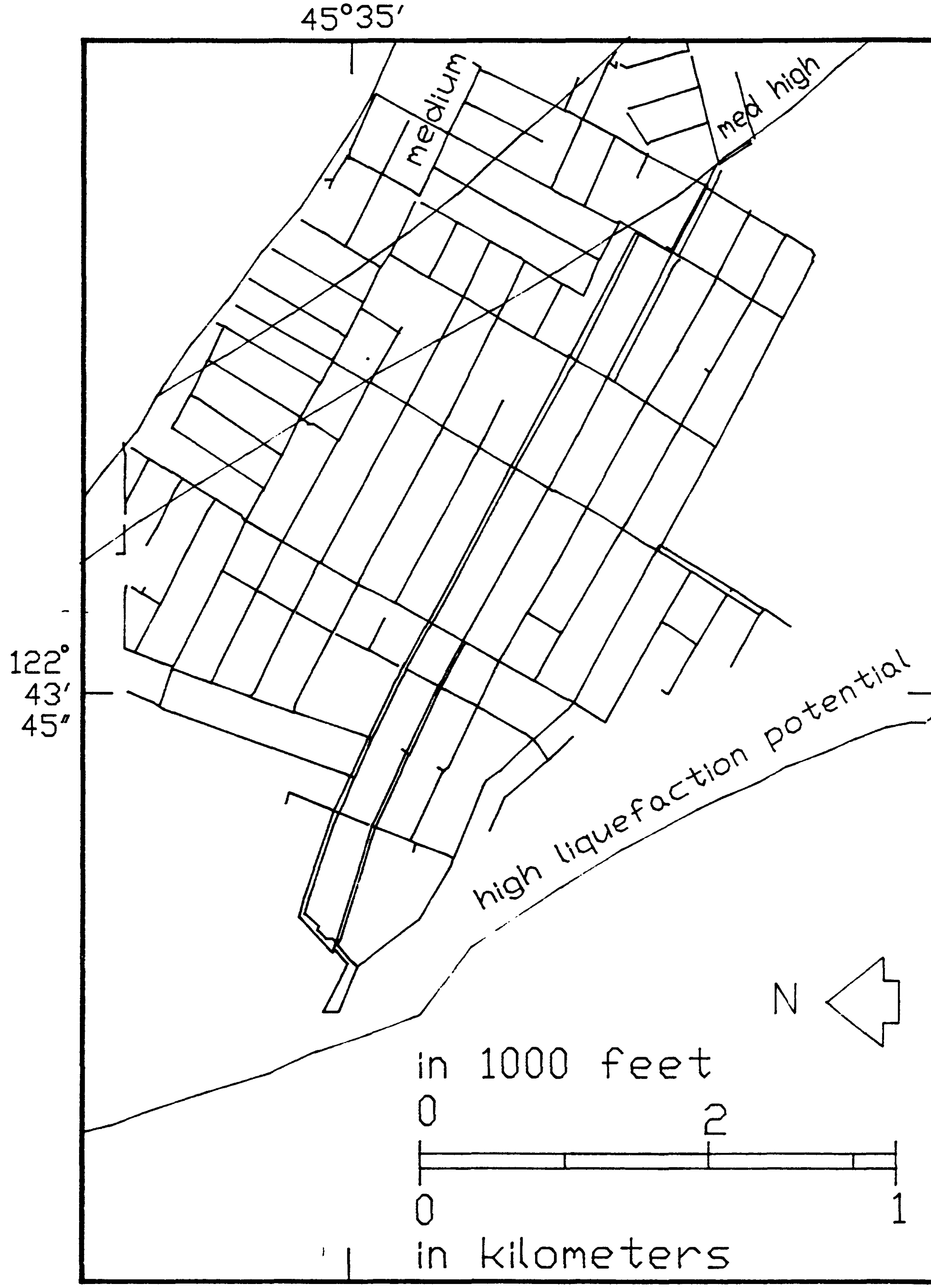

Figure 21. -- Fiske Drainage Basin Water Pipelines Damage Potential within Various Liquefaction Potential Zones under LES

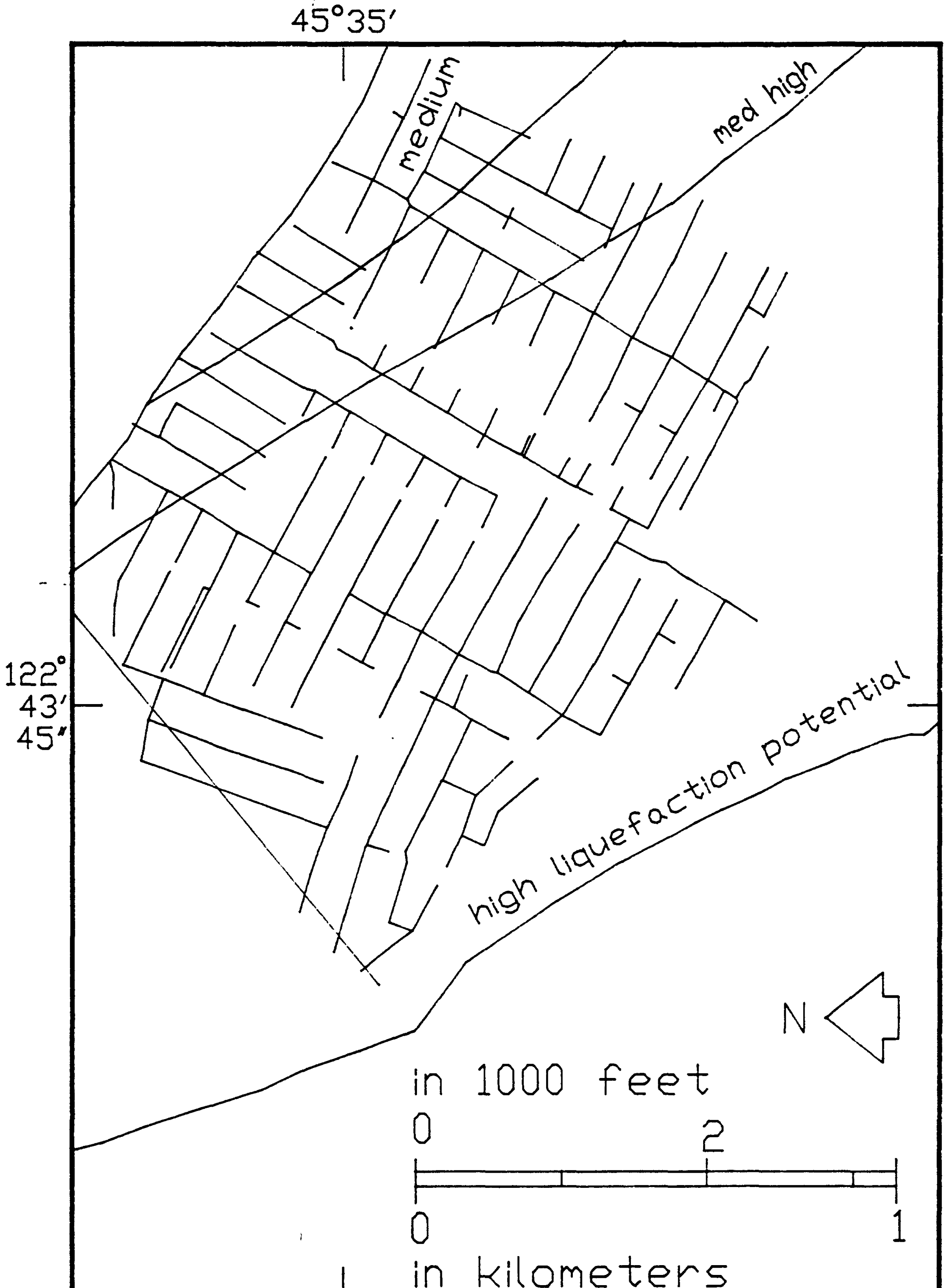

Figure 22. -- Fiske Drainage Basin Sewer Pipelines Damage Potential within Various Liquefaction Potential Zones under LES

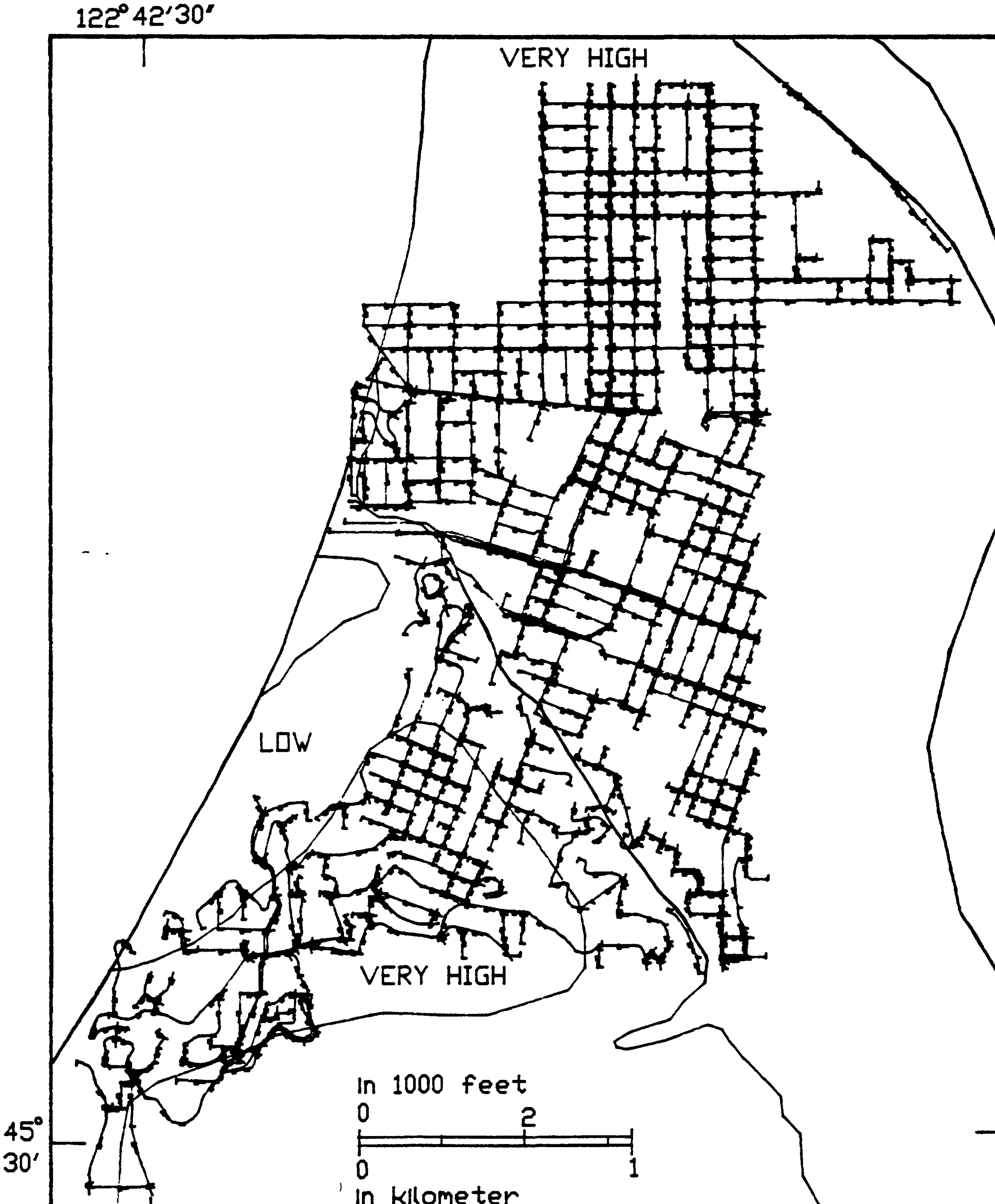

Figure 23. -- Tanner Drainage Basin Water Pipes Damage Potential within Various Liquefaction Potential Zones under SES

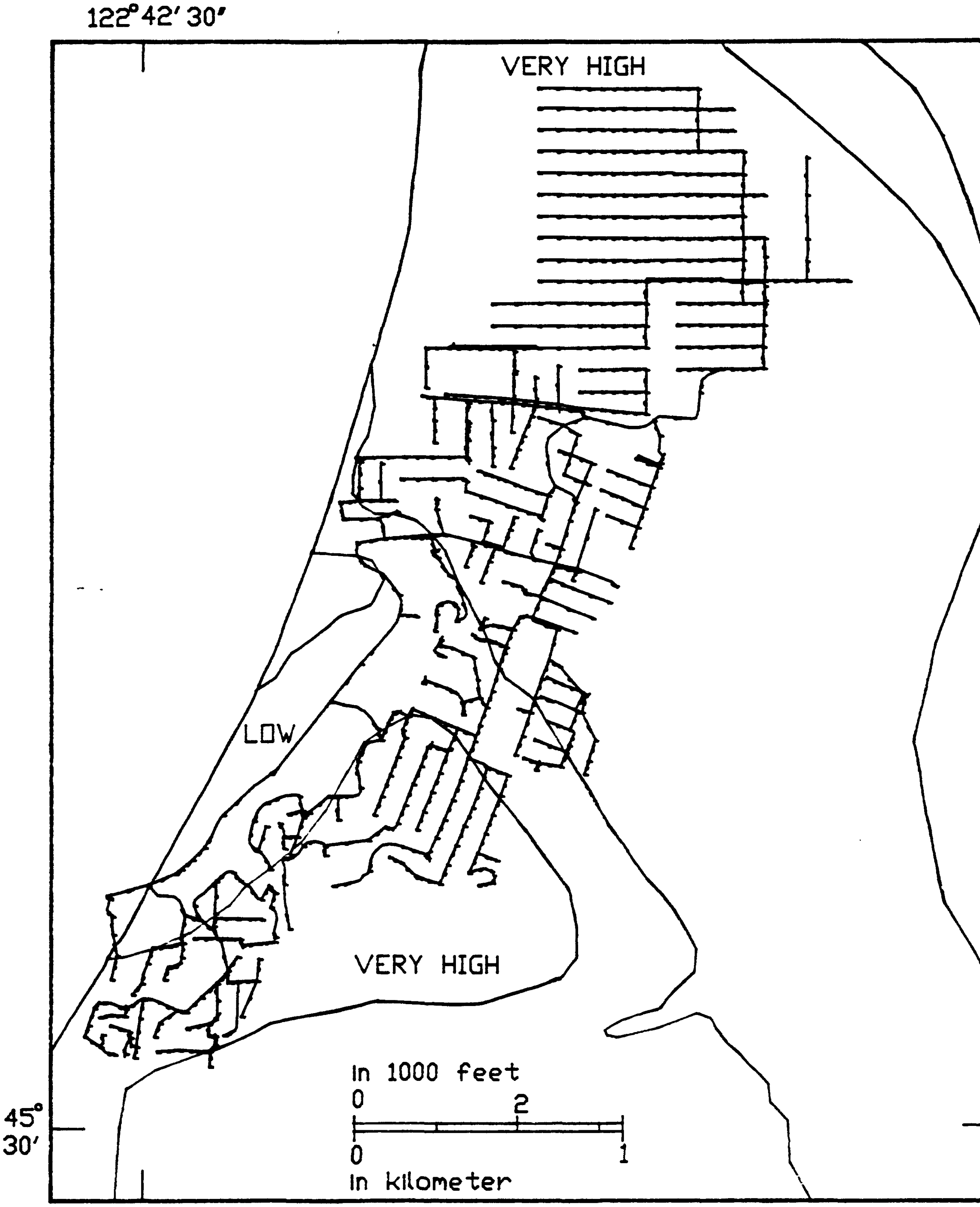

Figure 24. -- Tanner Drainage Basin Sewer Pipes Damage Potential within Various Liquefactio Potential Zones under SES

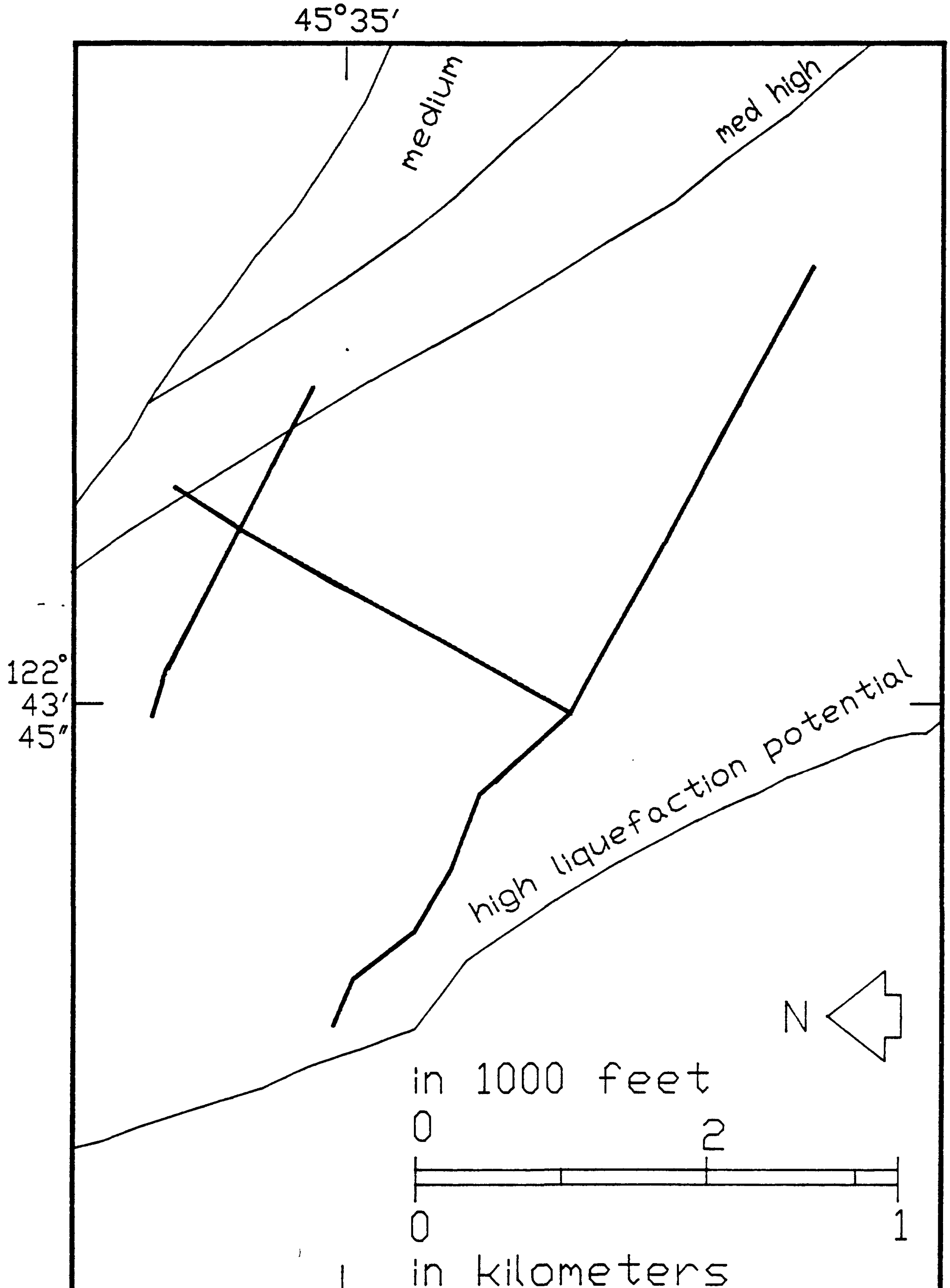

Figure 25. -- Cast Iron Pipes over 10" Diameter Installed prior to 1940

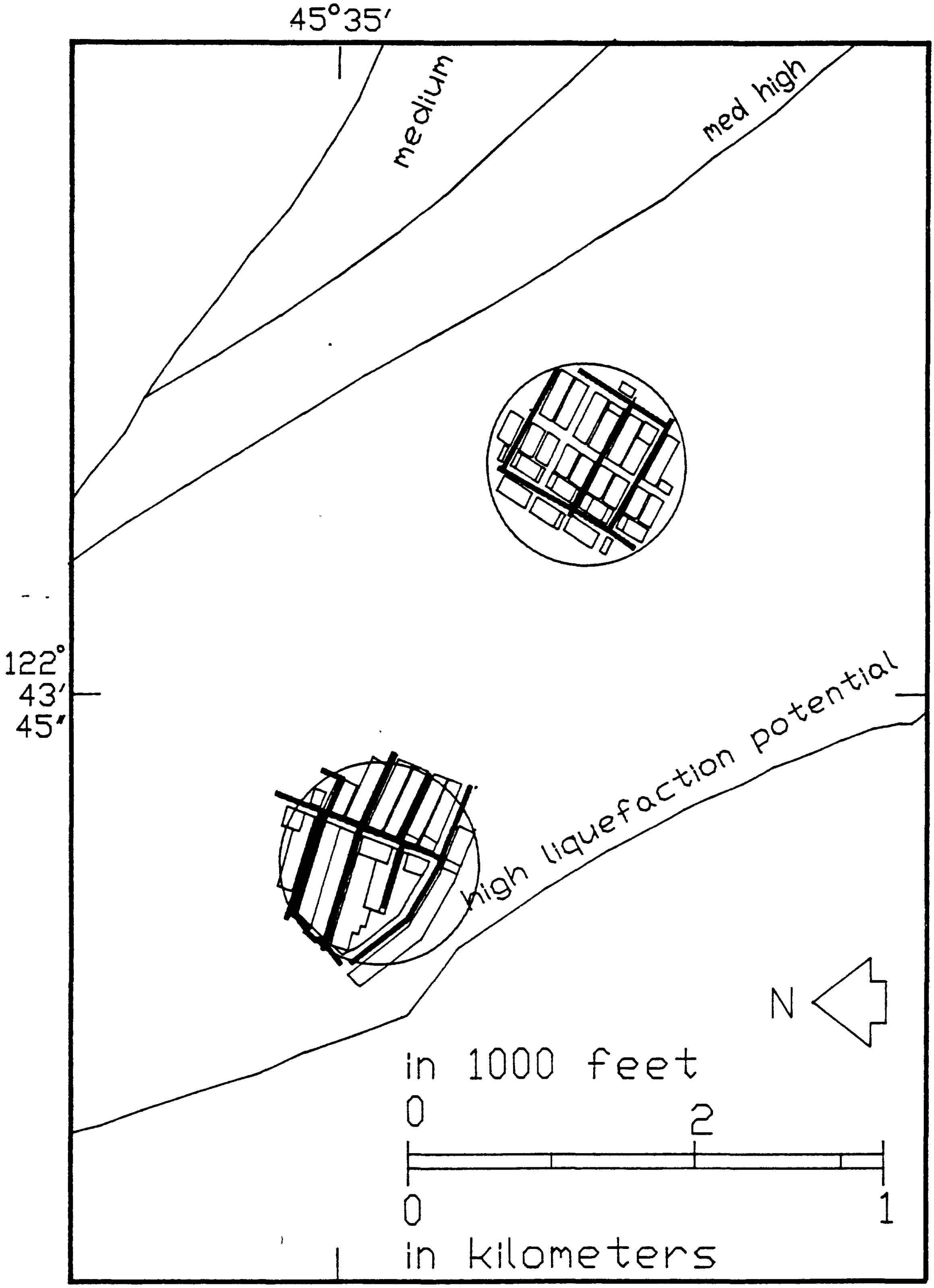

Figure 26. -- Pipes and Parcels with 750' Radius from a Water Problem Site.